UNIVERSITY OF VAASA

FACULTY OF TECHNOLOGY

ENERGY TECHNOLOGY

Anne Mäkiranta

DISTRIBUTED TEMPERATURE SENSING METHOD – USABILITY IN ASPHALT AND SEDIMENT HEAT ENERGY MEASUREMENTS

Master´s thesis for the degree of Master of Science in Technology submitted for inspection, Vaasa, 31 May, 2013.

Supervisor Erkki Hiltunen

Instructor Jukka Kiijärvi

ABBREVIATIONS AND SYMBOLS

Abbreviations

COP	Coefficient of performance
DTS	Distributed temperature sensing
GTK	Geological Survey of Finland
OM3	Optical multimode 3
PE	Polyethylene
PT100	Platinum resistance temperature sensor
RTD	Resistance thermometer detectors
UHI	Urban heat island

Symbols

C_+	Constant
C_-	Constant
c	Specific heat capacity [J/(kg·K)]
D	Distance [m]
E	Energy [J]
$I_+(z)$	Stokes band energy
$I_-(z)$	Anti-Stokes band energy
λ	Thermal conductivity [W/(m·K)]
$\Delta\alpha$	Attenuation [dB/km]
P	Power [W]
s^2	Variance
T_{ext1}	Temperature [°C]
$T(z)$	Temperature at the point z
t	Time [s]
u_A	Standard uncertainty

PREFACE AND ACKNOWLEDGEMENTS

This thesis is a part of the Geoenergy Research project at the University of Vaasa.

I started my studies in the field of Energy Technology in the autumn 2010 but actually I had started as an extra student in the previous spring on the course Physical Basics of the Energy Technology. On that course I heard about asphalt heat energy for the first time without a clue that it would be the topic of my thesis after a few years. Renewable energy has fascinated me all the way through this Master Degree Program and I am very grateful that I managed to get a topic related to geoenergy.

For the last one year period I have worked as a project researcher in the Geoenergy Research project and ReForm project at the University of Vaasa. During these projects I have been able to study geoenergy more precisely, meet some experts and get to know the companies in this field. One aim of the Geoenergy Research project is to explore the temperatures under the asphalt layer to understand how the heat from the Sun is transferred and stored in the soil. I have been working on that part starting from the beginning – how to measure temperature downwards regularly and accurately. This thesis gives the answer delving first into the theoretical background of the measurement method continuing to the practice both in the laboratory and in field conditions.

Thanks to my supervisor Research Manager Erkki Hiltunen and instructor Assistant Professor Jukka Kiijärvi for their support and help during my studies and thesis writing. Erkki Hiltunen has given me good advices on research of geoenergy. Jukka Kiijärvi has delivered his knowhow on heat transfer during my thesis writing. He has also given me answers to general research related questions. I would also like to address my thanks to our Professor Seppo Niemi who decided to accept me to this Master Degree Program. Even in an economist can live an engineer.

I would like to thank geoenergy expert Mr. Mauri Lieskoski who has helped me especially on the field of sediment heat energy. I would also like to express my gratitude to

Mr. Ilkka Martinkauppi from GTK Geological Survey of Finland. He has given me a number of good advices related to DTS measurement during my research work.

I would like to address my special thanks to all my work mates and especially to the research group of Renewable Energy. You have supported me and there has always been somebody who has had time to listen to my research related problems. We have a great team! Special thanks to Chemist Katriina Sirviö for acting as an assistant both in the laboratory and during the sediment heat measurements. There always was enough ice and warm sand. Most of all I appreciate her great and helpful attitude, despite the cold and windy weather on measurement days in Suvilahti. Special thanks also to Dr. Carolin Nuortila for critical reading and proposals for making this thesis more precise and legible. Thanks also to our best neighbor Mrs. Anja Viiru for the proofreading.

My warmest thanks go to my dear husband Mika and our lovely children Ella and Eetu. You have been patient and supported me although I have sometimes been studying even in the weekends. Let´s have a study free summer.

Vaasa 31.5.2013

Anne Mäkiranta

TABLE OF CONTENTS **page**

UNIVERSITY OF VAASA
Faculty of technology
Author: Anne Mäkiranta
Topic of the Thesis: Distributed Temperature Sensing Method – usability in asphalt and sediment heat measurements
Supervisor: Erkki Hiltunen (PhD)
Instructor: Jukka Kiijärvi (D.Sc. (Tech.))
Degree: Master of Science in Technology
Degree programme: Degree Programme in Electrical and Energy Engineering
Major of Subject: Energy Technology
Year of Entering the University: 2010
Year of Completing the Thesis: 2013 **Pages:** 65

ABSTRACT

Geoenergy consists of both geothermal energy from the ground and the radiant energy of the Sun. Geoenergy is available in ground, bedrock, watercourses, sediment and asphalt. Asphalt and sediment heat and the exploitation of these are research areas of the Geoenergy- project at the University of Vaasa in the Faculty of Technology. There was a need for additional knowledge about the behavior of the heat under the asphalt and in the sediment. That is why the temperatures were needed to be monitored regularly in those layers.

In this thesis the possibility of the utilization of the Distributed Temperature Sensing (DTS) method in asphalt and seabed sediment heat measurements was explored.

The utilization of the Distributed Temperature Sensing method in asphalt heat measurements was explored in the laboratory. At the same time the new optical DTS-method based device was taken into use and its features were introduced. In the laboratory measurements the features of the device and the cable was explored and the uncertainty of measurement was defined. The temperature of the sediment was measured in field conditions in Suvilahti, Vaasa. The field measurements gave information about the stage of the sediment heat temperature in the low-energy network in Suvilahti. Results were compared to previous data measured at the same place a few years ago. The sediment heat measurements will be continued regularly.

The conclusion of the results is that the Distributed Temperature Sensing method is an accurate and diverse method to utilize in asphalt and sediment heat measurements. The method performs well both in the temperature measurements under the asphalt layer and in the monitoring of sediment heat temperatures.

KEYWORDS: Distributed Temperature Sensing, Geoenergy, Urban Geoenergy, Urban Heat Island, Asphalt heat, Seabed Sediment Heat

VAASAN YLIOPISTO
Teknillinen tiedekunta
Tekijä: Anne Mäkiranta
Diplomityön nimi: Hajautettu lämpötilanmittausmenetelmä – käytettävyys asfaltti- ja sedimenttilämmön mittaamisessa
Valvojan nimi: Erkki Hiltunen (FT)
Ohjaajan nimi: Jukka Kiijärvi (TkT)
Tutkinto: Diplomi-insinööri
Koulutusohjelma: Sähkö- ja energiatekniikan koulutusohjelma
Suunta: Energiatekniikka
Opintojen aloitusvuosi: 2010
Diplomityön valmistumisvuosi: 2013 **Sivumäärä:** 65

TIIVISTELMÄ

Geoenergia koostuu maan sisältä tulevasta geotermisestä energiasta ja auringon säteilyenergiasta. Geoenergiaa on saatavilla maasta, kallioperästä, vesistöistä, sedimentistä ja asfaltista. Asfaltti- ja sedimenttilämpö sekä niiden hyödyntäminen kuuluvat Vaasan yliopiston Teknillisen tiedekunnan Geoenergia-projektin tutkimusaiheisiin. Lämpöenergian käyttäytymisestä asfaltin alla ja sedimentissä tarvittiin lisätietoa, joten näiden kerrosten lämpötiloja oli pystyttävä mittaamaan säännöllisesti.

Tässä diplomityössä selvitettiin mahdollisuutta hyödyntää hajautettua lämpötilanmittausmenetelmää (Distributed Temperature Sensing, DTS) asfaltin alaisten maakerrosten lämpötilan mittauksessa ja merenpohjan sedimenttilämmön mittauksessa.

Hajautetun lämpötilanmittausmenetelmän hyödyntämistä asfalttilämmön mittauksissa tutkittiin laboratorio-olosuhteissa. Samalla uusi optinen DTS-menetelmään perustuva mittauslaite otettiin käyttöön ja sen ominaisuuksiin tutustuttiin. Laboratoriomittauksilla selvitettiin laitteen ja kaapelin ominaisuuksia sekä määritettiin mittausepävarmuus. Sedimentin lämpötila mitattiin maastossa Vaasan Suvilahdessa. Maastomittaukset antoivat tietoa Suvilahden matalaenergiaverkon sedimenttilämpötilan tasosta. Sedimentistä saatuja lämpötilakäyriä verrattiin muutaman vuoden takaisiin mittauksiin samasta paikasta. Sedimentin lämpötiloja aiotaan mitata jatkossa säännöllisesti.

Tämän diplomityön tuloksista voidaan päätellä, että hajautettu lämpötilanmittausmenetelmä (DTS) on tarkka ja monipuolinen menetelmä käytettäväksi asfaltti- ja sedimenttilämmön mittaamisessa. Menetelmä soveltuu hyvin sekä asfaltin alaisten kerrosten lämpötilan tutkimuksiin että sedimentin lämpötilojen seurantaan.

AVAINSANAT: Hajautettu lämpötilan mittaus (DTS), geoenergia, urbaanigeoenergia, asfalttilämpö, sedimenttilämpö

1. INTRODUCTION

This thesis is a part of the Geoenergy Research project (2011–2014) at the University of Vaasa, Faculty of Technology. One aim of the project is to explore the temperatures under the asphalt layer to understand how the heat from the Sun is transferred and stored in the soil. The question how the collection of the heat should be performed must also be solved. However, the first problem to solve is how the temperatures shall be measured. It is expected to get results with approximately 10 cm distances downward during under at least a one year period. The climate conditions especially frost has to be taken into account when deciding on the solution.

After one month exploring and discussing with experts in this field, the measurement system was chosen among a few possibilities: thermocouples detectors, temperature sensors, thermistors, platinum resistance thermometer detectors (RTD) and distributed temperature sensing (DTS) method. The DTS method was seen as modern, multipurpose and accurate method for temperature monitoring in geoenergy projects. The DTS method is based on backscattering of light. Optic fiber cable functions as a linear sensor monitor temperature. Temperatures can be measured as a continuous profile along the whole fiber not only at points. In other words temperature measurement is distributed. An Oryx DTS device was acquired to the Faculty of Technology in the autumn 2012.

In the beginning of this thesis the terms geothermal energy, geoenergy, asphalt and sediment heat are introduced. However the main point of this thesis is to introduce the theory of the distributed temperature sensing (DTS) method, to test it in practice and to evaluate the results. In the Faculty of Technology the DTS method is first utilized to monitor temperatures in seabed sediment and soil under the asphalt layer. The DTS method shall later be used in bedrock energy wells in geoenergy related projects. However, this thesis is outlined to introduce the DTS method, test it and install the device. Regular and continuous monitoring of temperatures in seabed sediment is started and documented as a part of this thesis also.

The DTS-measurement device had to be tested first. The test measurements were made in a laboratory. The test arrangements are described and the results are presented. The second task was to perform measurements of the sediment temperature in the House Fair 2008 area in Suvilahti, Vaasa. These measurements will be the start for continuous monitoring of temperatures in the seabed sediment in Suvilahti.

At the end of the thesis the results are presented and discussed. The results from the seabed sediment measurements are being compared to findings made by the Geological Survey of Finland. In the conclusions chapter the success of the research is evaluated and the further research subjects are proposed. The whole thesis is summarized in the end.

The aim of the thesis is the installation of the new DTS device, testing its usability in asphalt and sediment heat measurements and evaluation of the results.

The scope of the research is outlined to consider asphalt condition measurements only in laboratory and at the same time explore the new device and its functions. The sediment heat measurements will be executed in real conditions in Suvilahti instead.

2. GEOTHERMAL ENERGY AND GEOENERGY

Geothermal energy consists of all energy sources under the Earth´s surface. Geoenergy instead consists of both geothermal energy and radiant energy from the Sun shown in Figure 1.

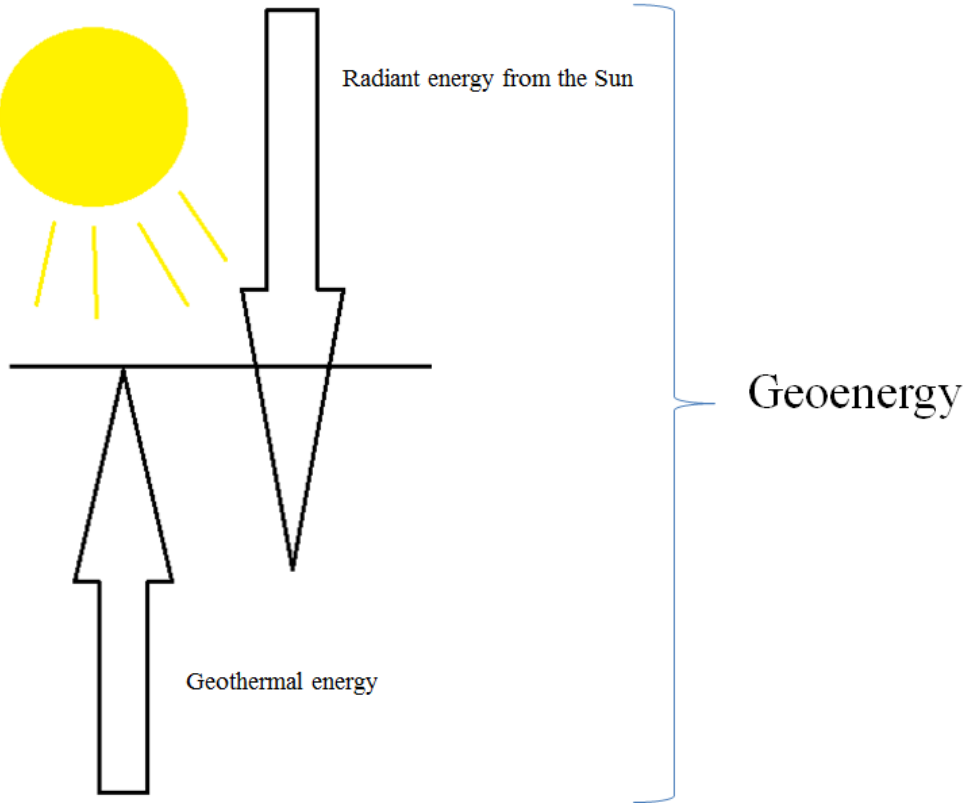

Figure 1. Geoenergy consists of geothermal energy and radiant energy emitted by the Sun.

Geothermal energy arises in many ways. Firstly the liquid mass erupting from the outer core of the Earth sets free thermal energy. This occurs as earthquakes and hot wells in volcanic areas. In other words, the continuous cooling of the Earth relieves heat. However, the main source of geothermal energy is the decay of long-lived radioactive isotopes. (Lowrie 2007: 221.)

Part of the radiant energy from the Sun is stored in the upper layers of the Earth. That energy is called ground source heat and it is one form of geoenergy. On the other hand, water system´s heat, seabed sediment heat, bedrock heat and asphalt heat are also different forms of geoenergy. The most important geoenergy form for mankind is the radiant energy emitted by the Sun and stored in the upper layers of the Earth. (Geoenergia.fi 2010.)

The geothermal resources of the Earth are enormous. It is estimated that the geothermal energy in the depth of 3 km is 43 000 000 EJ (1 EJ=10^{18} J), which means 1 194 444 444 TWh (1 TWh= 10^{12} Wh). If a small part of this energy could be converted into electric power, the total world net electricity generation, which is expected to grow to reach 30 364 TWh in the year 2030, could be covered easily. (Chandrasekharam & Bundschuh 2008:13.)

Low-enthalpy resources have neither been exploited efficiently in developing countries nor in industrialized countries. It is still believed that it is impossible to generate electric power by ground source heat economically. (Chandrasekharam & Bundschuh 2008:15.) In volcanic areas geoenergy is mostly utilized in generating electricity and for heating and cooling of houses in non-volcanic regions. (Aswathanarayana, Harikrishnan & Sahini 2010: 46.)

In the Earth´s core the temperature is still approximately 5000 °C (± 2000 °C) (Ahvenisto, Borén, Hjelt, Karjalainen & Sirviö 2004: 31.) The volcanic lava can reach the temperature of 1200 °C and thermal springs can achieve 350 °C. The Earth receives as much energy from the Sun in only 30–40 minutes as humankind uses in a year. (Lipták 2009: 64, 77.) The geoenergy which arises from the radiant energy of the Sun can be divided according to the source from it is gathered as follows: ground source heat, bedrock heat, watercourse thermal heat, sediment heat and asphalt heat. These are the most commonly used forms of geoenergy in non-volcanic areas.

According to Leppäharju (2008) the influence of the radiant energy from the Sun reaches to the depth of 10 m in Finland. As a consequent of this bedrock heat consists of both solar energy and geothermal energy.

2.1. Climate and Weather Conditions in Finland

Evidently, the climate has an influence on the quantity of heat gathered from the Sun. In Finland an intermediate climate is prevailing which includes both characteristics of a maritime and a continental climate. The weather depends highly on the prevailing wind direction and the location of low and high pressures. The weather varies quickly particularly in the winter because of the country´s location in the zone of prevailing westerly winds, where tropical and polar air masses meet. Typically south-west air flow is common in Finland.

According to the Finnish Meteorological Institute (2010) the annual mean temperature varies from a couple of Celsius degrees of frost in Northern Lapland to more than +5 °C in southwestern Finland. The mean temperature of Finland is higher than in other countries at the same latitude. For instance, in Siberia and in Greenland temperatures can be 20–30 degrees lower in the winter time. The main reason for Finland having higher temperatures is the North Atlantic current resulting from the Gulf Stream and having an effect up to the Arctic Sea. Additionally the Baltic Sea and thousands of inland water bodies are heating the Finnish climate.

The annual amount of rainfall is approximately 500–650 mm. The largest amount of precipitation is measured in Southern Finland and in the central part of Finland and the least amount of precipitation is measured in Lapland. The radiant energy emitted by the Sun amounts to 1000 kWh/m² annually in Finland (Finnish Meteorological Institute 2010). There are four distinct seasons and in Northern Finland almost half of the year is dominated by winter. Snow cover has an impact on ground temperature while it is acting as an insulating layer. The frost in the ground also has to be taken into account in geoenergy related research.

2.2. Geological Conditions in Finland

Geological conditions have an effect on the amount of heat energy in asphalt and sediment. Finland is located in a non-volcanic area and the heat flow from the Earth´s core is only 60–85 mW/m^2 on an average, while for example in Iceland it is 85–120 mW/m^2. The bedrock of Finland consist mainly of granite, gneiss related rocks and also of greenstone which post-dates the powerful volcanic age 2800 million years ago (Ahvenisto et al. 2004: 22, 34).

The ice age has formed the North European landscape so that there cannot be found such a humus layer like in the Central Europe. The rock heat is easily usable in Finland. The amount of heat capacity gathered from the rock is dependent on the consistency of the bedrock and quality of soil. Especially the groundwater and it`s flow are important things to take into account while approximating the heat flow in the bore hole. According to Rosen, Gabrielsson, Fallsvik, Hellström and Nilsson (2001: 40) the more rough-grained the soil is the higher the permeability is and the quicker the ground water flows through.

2.3. Asphalt heat

Asphalt pavements gather solar heat and bind a significant quantity of energy at the same time. A part of that energy conducts to underlying layers of asphalt. According to Qinwu & Mansour (2010) the specific heat of asphalt concrete is 920 J/(kg·°C) measured as an average of several mixtures. Asphalt heat can be gathered by collector pipes with liquid circulation located under the pavement. The heat is then led to thermal storages e.g. under a building and it is utilized in the building during winter with the help of a heat pump via a floor heating system. Asphalt heat energy can also be exploited for keeping footpaths and parking lots unfrozen around the year see Figure 2. (ICAX 2012).

Figure 2. A parking lot is kept unfrozen in winter by using asphalt heat. (ICAX 2012).

Asphalt heat is a form of urban energy – urban geoenergy. According to Allen, Milenic & Sikora (2003) the urban heat island (UHI) effect is based on the built environment and lack of flora. Buildings, surface materials like rock and concrete and asphalt pavements absorb sunlight effectively. The other reason that strengthens in the phenomenon is the lack of evaporation of soil moisture and transpiration from vegetation. Researchers Canbing, Jincheng & Yijia (2010:3) have come to the conclusion in their research that the urban heat island effect feeds itself. So the best energy saving potential can be reached by mitigating UHI effect. Santamouris (2003:215) also sees the use of energy supply systems, which utilize renewable energy sources for buildings, as one solution in the battle against urban warming.

2.4. Seabed sediment heat

Sediment heat can be gathered from the sediment layers in the bottom of different water courses. Sediment is a solid matter layer consisting of clay, mud and gyttja. There are thick sand layers in the coastline of Finland and plenty of sediment in shallow bays.

In the Vaasa Housing Fair 2008 a new energy solution was introduced: low-energy networks for seabed sediment. A total amount of 43 single-family houses were connected to the heat distribution network. The collector pipework was drilled in 3–4 meters depth measured from the sea level. Nevertheless, the network is also used for cooling houses in the summertime. (Panula 2008.)

The Low-energy network utilizes low temperatures to produce heat for apartments. Figure 3 shows how the low temperature heat collection pipe works. These kinds of pipes are assembled to the Suvilahti seabed sediment.

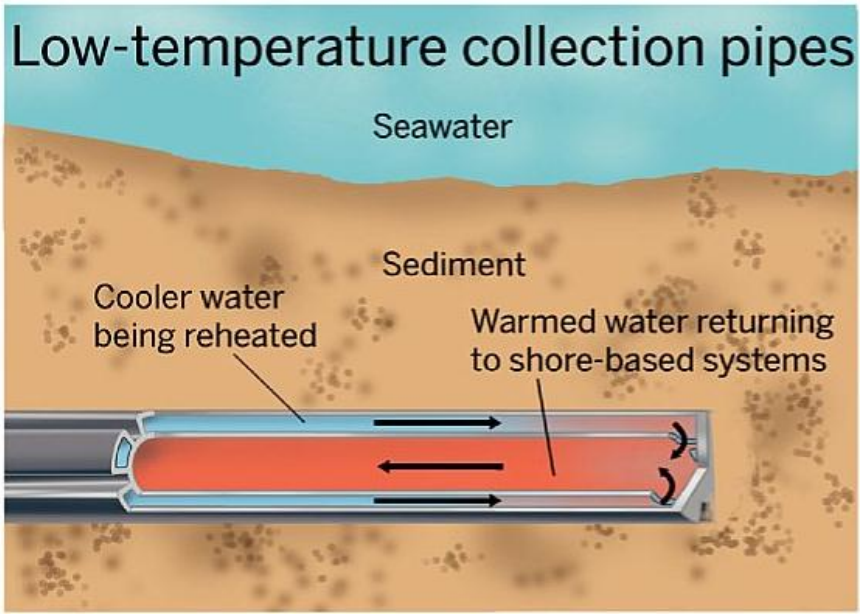

Figure 3. The function of the low temperature heat collection pipe in the sediment layer. (By courtesy of Mauri Lieskoski 2013).

According to Martinkauppi (2010) the Geological Survey of Finland has measured temperatures of 8–9 °C in the seabed sediment around Ostrobothnia and South Ostrobothnia from about 3–5 meters depth. The hard and stony soil can be seen as a restriction for the exploitation of sediment heat. (Geoenergia.fi 2010.)

Measurement results in the Suvilahti seabed sediment from 2006 are shown in Figure 4.

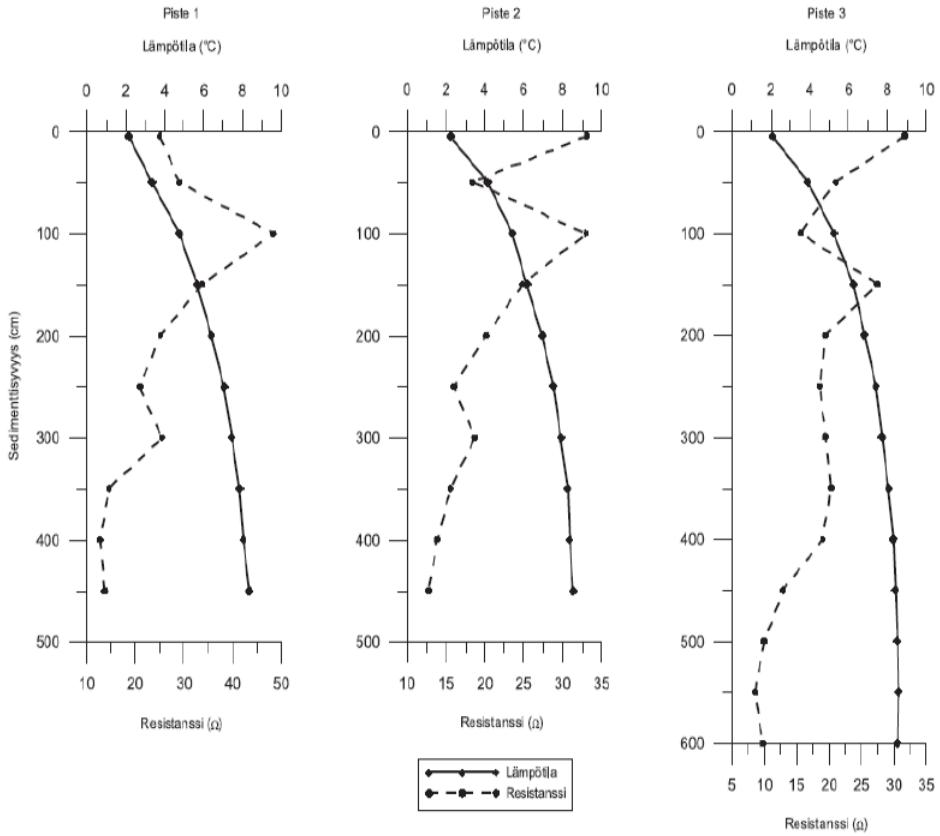

Figure 4. Temperature and resistance measurement results in the Suvilahti seabed sediment in April 2006. (Valpola 2006).

The temperature profile measured along a borehole (Figure 5) shows lower temperature in 3–5 m depth than in the sediment. Apparently, the temperature in seabed sediment is higher than in boreholes at same depths.

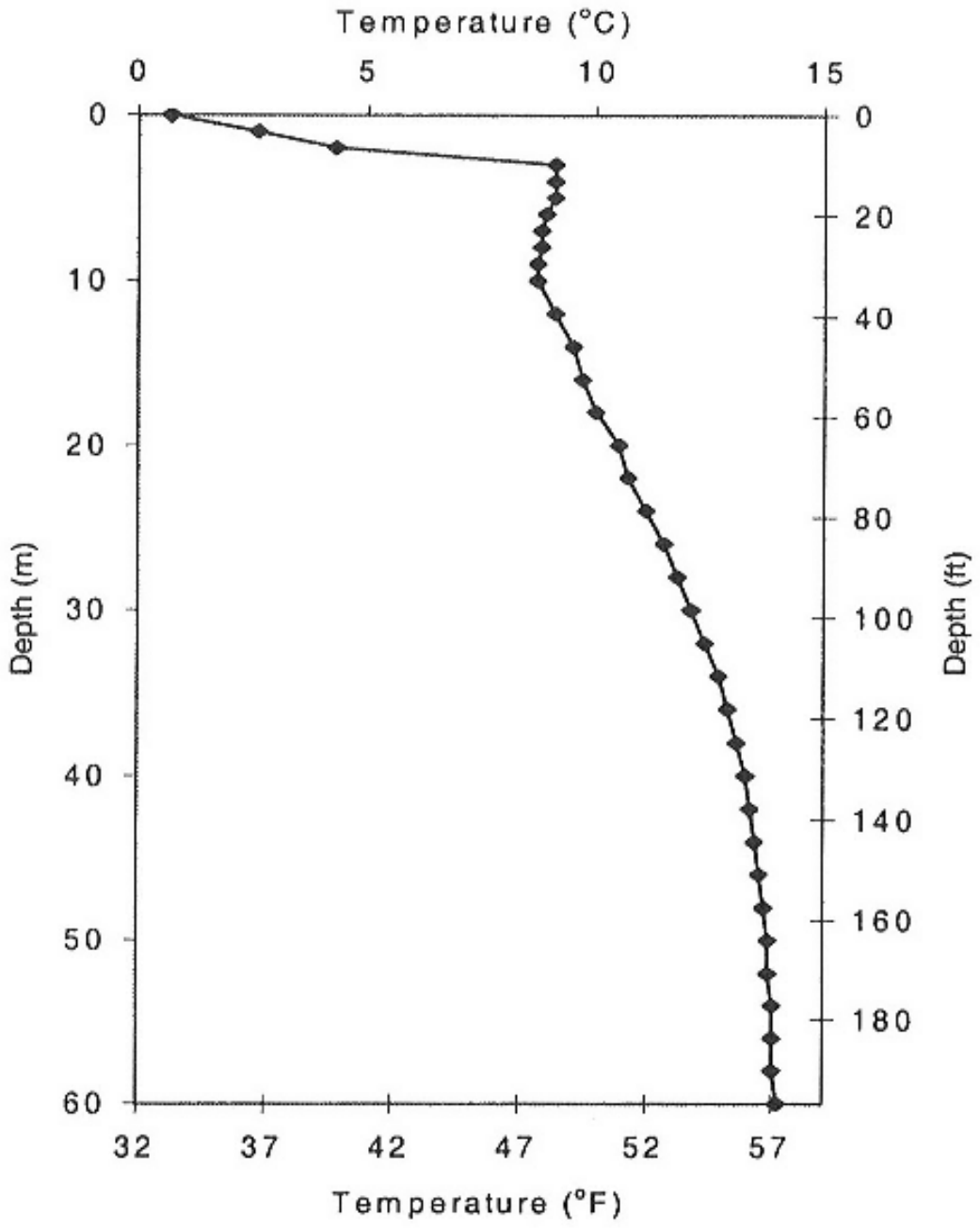

Figure 5. Temperature profile along the borehole. (Gehlin & Nordell 2003).

3. THEORY OF DISTRIBUTED TEMPERATURE SENSING METHOD

Distributed temperature sensing (DTS) is a method for temperature measurement, where optical fiber functions as a linear sensor. Temperatures can be measured as a continuous profile along the whole fiber, not only at points. In other words temperature measurement is distributed. The fibers, which are typically made from doped quartz glass, can be even several kilometers long.

The DTS-measurement device emits short pulses of laser light, to illuminate the glass core of an optical fiber seen in Figure 6. Part of the incident light pulse is backscattered while it moves along the core of fiber. The intensity of these backscattered bands is acquired by the DTS-measurement device. The device estimates the temperatures based on the temperature dependent part of scattering. (LIOS Technology 2012, Sensornet 2007, Englund, Mitrunen, Lehtiniemi & Ipatti 2008: 5–6.)

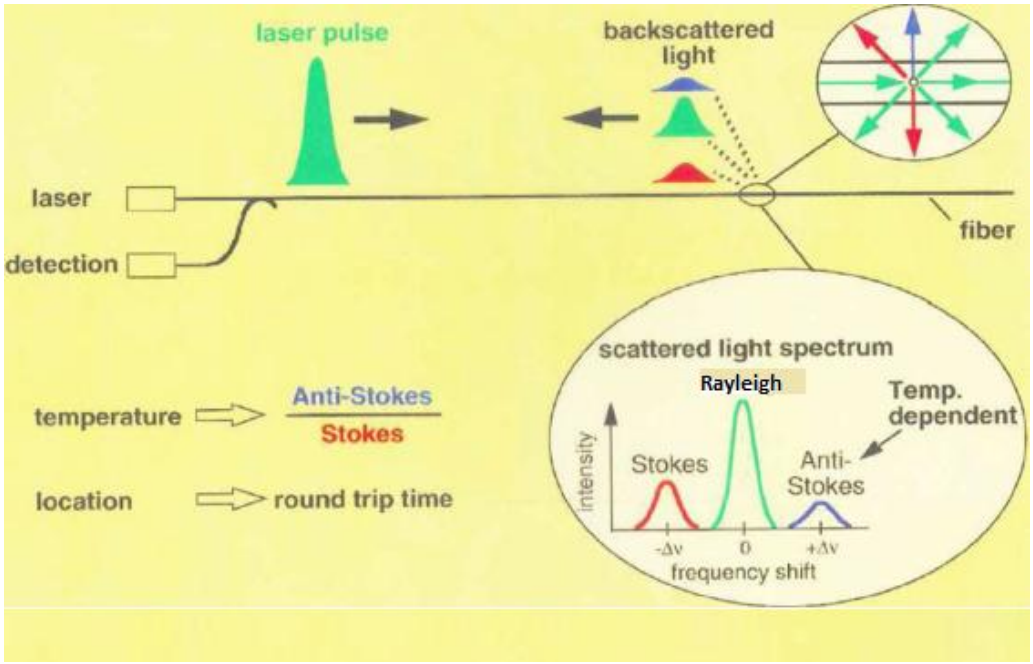

Figure 6. The operating principle of the distributed temperature sensing method. (Ukil, Braendle & Krippner 2012: 885.)

3.1. Backscattering light

There are two types of scattering involved in the DTS technology, the Rayleigh scattering and the Raman scattering. The DTS-device emits short laser pulses which are partly backscattered. The natural density fluctuations of the glass core are the major cause for scattering radiation, called Rayleigh scattering. It can be used to get information on the optical loss of the fiber and it is used in OTDR (Optical Time Domain Reflectometer) measurements. The Rayleigh scattering is not sensitive to temperature but it is used in calibration of the DTS device. (LIOS Technology 2012, Sensornet 2007, Englund, Mitrunen, Lehtiniemi & Ipatti 2008: 5–6.)

Most photons are elastically scattered (Rayleigh scattering) having the same kinetic energy as the incident photons. A small portion of scattered photons are scattered with an excitation having different frequency than incident photons. Raman scattering is that kind of inelastic scattering of a photon. Raman scattering is more important for DTS measurements than the Rayleigh scattering since it is temperature dependent. Temperature affects the amorphous solid structure of the glass fiber and induces lattice oscillations within the solid. The photons interact between the electrons of the molecule when incident light falls on to thermally excited molecules. This interaction results in the backscattering of light, which undergoes a spectral shift and the frequency of the photons is slightly changed. The spectral shift is equivalent to the resonance frequency of the lattice oscillation (LIOS Technology 2012, Ukil et al. 2012: 885.)

The Raman signal comprises Stokes and anti-Stokes bands. When photons lose their energy to the glass fiber their frequency is downshifted and they are known as Stokes photons. On the other hand, the frequency of the photons increases as they gain energy from the glass, resulting in anti-Stokes photons. Eventually both of these photon types are traveling along the fiber to be detected by the DTS measurement device. However, anti-Stokes band intensity is dependent on temperature while the Stokes band intensity is not. The DTS system estimates the temperature locally in different distances by means of the ratio of anti-Stokes and Stokes band intensities and the delayed time of

optical pulse shown in Figure 6. (Quimby 2006: 60–61, LIOS Technology 2012, Sayde et al. 2010: 1, Sensornet 2007.)

The temperature T(z) can be evaluated by Equation 1 where T is temperature, z is the distance, $\Delta\alpha$ is the attenuation, C_+ and C_- are constants, $I_+(z)$ is Stokes band energy and $I_-(z)$ is Anti Stokes band energy.

$$T(z) = T_{ref}\left(1 + \frac{\Delta\alpha z}{\ln\left(\frac{C_+}{C_-}\right)} + \frac{\ln\left(\frac{I_+(z)}{I_-(z)}\right)}{\ln\left(\frac{C_+}{C_-}\right)}\right) \quad (1)$$

This equation is a simplification where the first term represents the offset, the second term the differential attenuation and the third term the temperature measured from the anti-Stokes to Stokes ratio. (Smolen & van der Spek 2003: 6.)

3.2. Fibers used in DTS measurements

Optical fibers are typically made of doped quartz glass. There exist two kinds of optical fibers, single mode and multimode types. The multimode means that the optical fiber can guide multiple modes of light along the fiber core. The multimode fiber gives better signal levels for DTS devices compared to a single mode fiber. The single mode fibers are commonly used in telecommunications. (Sensornet 2007).

The absorption, radiation scattering and reflection cause a marginal loss of signal in all optical fibers. This results in the Stokes and anti-Stokes signals showing an exponential decay with distance. The splices and connectors or even breakage in the fiber cause step loss points. The overall loss of signal is expressed by an attenuation coefficient which is wavelength dependent. (Sensornet 2007).

An optical fiber consists of the core which is surrounded by an outer cladding (Figure 7). This is called bare fiber. The core diameter of fibers used in DTS measurement in this thesis is 50 µm and the cladding diameter is 125 µm. The bare fiber is surrounded by the primary coating which prevents mechanical damages to the core and the cladding. The primary coating can be made of acrylate with a diameter of 250 µm for example.

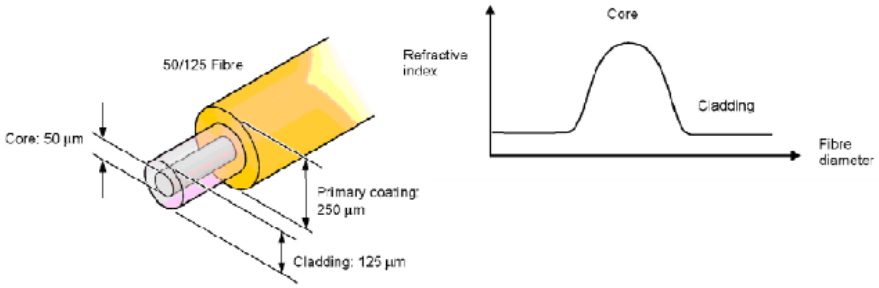

Figure 7. The construction of an optical multimode fiber. (Sensornet 2007).

4. METHODS

The implementation and testing of a brand new Oryx DTS device was arranged at the Technobothnia Research Centre in Vaasa. There was also an intention to measure in real conditions with the Oryx DTS device. The House Fair 2008 area in Suvilahti in Vaasa offers a great opportunity for this purpose, because of the already existing cables in the sediment.

4.1. Testing and laboratory measurements in Technobothnia

Laboratory measurement arrangements in an experimental situation were carried out at the Technobothnia Research Centre. The scope was to investigate below ground conditions both during the summer and winter seasons (Figure 8). The main idea was to make a clear temperature gradient in two measurement set-ups in order to test the functions of the DTS device. The third set-up demonstrated the dry summer conditions on asphalt surface and gravel and sand layers under it.

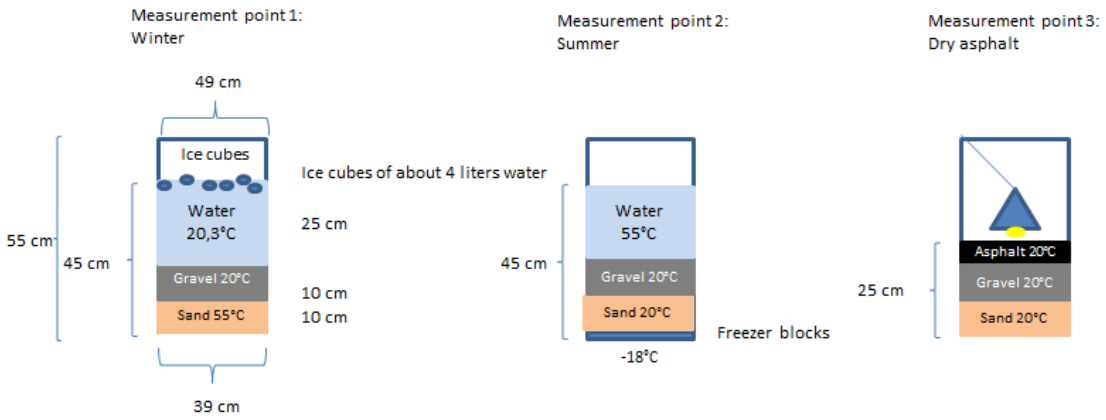

Figure 8. Experimental set-up. Materials used and temperatures in the beginning of measurement.

The measurement points were built up using plastic tubs by the volume of 80 liters. Three tubs were filled with different mixture of sand, gravel, asphalt, water and ice cubes. First, the cable with the optical fibers was centralized in the tubs vertically. The 50/125 µm multimode, OM3 (Ultra-Fox Plus) cable was wound round a skeleton frame made of hexagon net shown in Figure 9.

Figure 9. Tub viewed from above.

The total length of the cable was 525 m. There were two fibers inside the cable spliced together at the end of the cable, which makes the total length of 1050 m of fiber. This U-installation actually gives two temperature values for each point of cable (Figure 10). A total of 70 m cable was wound around the skeleton frame up to a height of 50 cm from the bottom in each tub. 1,4 m of wound cable was equivalent to 1 cm height in the tub. The cable was led consecutively through all three tubs. The set-up is illustrated in Figure 10.

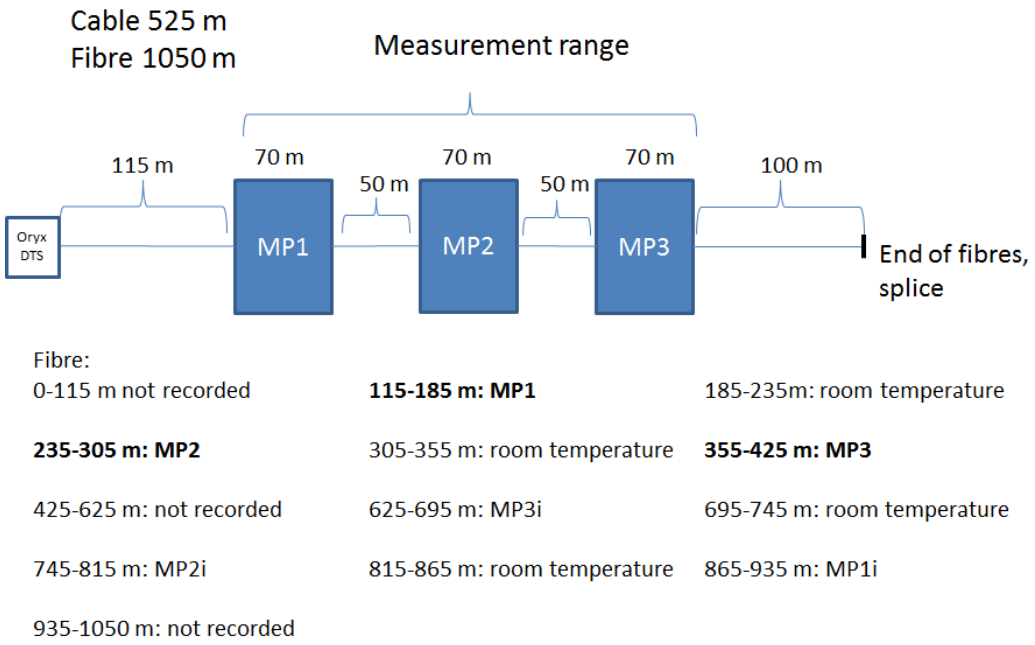

Figure 10. The measurement arrangements in double-ended measurement. Only Measurement Points (MP) 1, 2 and 3 are taken into account.

Due to the results of estimation of uncertainty (chapter 4.2.) it could be decided that in the following inspections of results only one fiber was taken into account and especially measurement points 1, 2 and 3 were noticed.

Finally, the tubs were insulated with cellular plastic Nomalen 30 (PE 30kg/m^3) seen in Figure 11. Thermal conductivity of Nomalen 30 is 0,038 W/(m·K) and thickness is 15 mm. (NMC Cellfoam Oy 2013.)

Figure 11. Three insulated measurement tubs.

The Oryx DTS device by Sensornet was used in all measurements executed in this thesis. The function of Oryx is based on Raman scattering. The accuracy of temperature measurements is ± 0,5 °C as given by the manufacturer. Room temperature in the laboratory was measured by PT100 platinum resistance temperature sensor, the accuracy of which is ± 0,25 °C.

In the measurement configurations the spatial resolution was set to 1 m. In other words, temperatures could be located for 1 m accuracy of the whole length of cable. In the measurement configurations two channels were used, the measurement time was set for 5 minutes per channel and 6 measurements per hour were executed. The following Table 1 summarizes the materials and the temperatures in which the respective cablemeters were embedded.

Table 1. Overview of the measuring point tubs with the multimode cable distances and their respective positions within the filling material.

MP1: (m)	Winter
115–129	sand 55°C
129–143	gravel 20°C
143–178	water 20,3°C
177–178	ice cubes 0°C

MP2: (m)	Summer
235–236	hard ice packs
236–249	sand 20°C
249–263	gravel 20°C
263–298	water 55°C

MP3: (m)	Dry asphalt
355–369	sand 20°C
369–383	gravel 20°C asphalt
383–390	20°C
390–408	lamp heat
408–409	60 W bulb

Measurements started on 14.1.2013 at 15:13 in MP1 and at 15:55 in MP2. MP3 was got ready on 15.1.2013 at 8:16. Measurement points 1 and 2 were monitored as long as their temperatures stabilized to room temperature. The MP3 dry asphalt tub was measured for a 6 days period, heating the layers above with a 60 W bulb during the first 4 days, 5–7 hours per day. Measurement arrangements of the MP3 dry asphalt tub are shown in Figure 12. The asphalt layer consisted of asphalt discs with a diameter of 10 cm and a height of 5 cm.

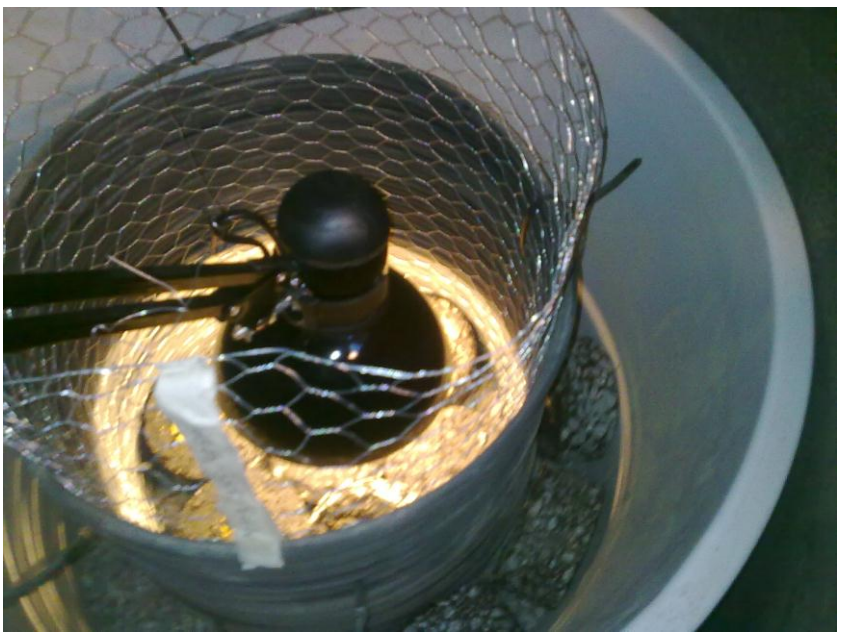

Figure 12. Measurement arrangements inside the MP3 dry asphalt tub.

Heat capacity and thermal conductivity of the materials that were used in measurements, are presented in Table 2. The values for this table have been collected from different sources.

Table 2. Some physical properties of materials used in measurements. (Earth energy Designer-program EED 2012, Valtanen 2007:349–350, 353, Qinwu&Mansour 2010:487.)

	Heat capacity [kJ/kg·K]	Thermal conductivity [W/m·K]
Air	1,005	0,025
Ice (0 °C)	2,10	2,25
Water (20 °C)	4,18	0,598
Sand (dry, 20 °C)	0,84	0,35
Sand (saturated)	1,5	2,40
Gravel (dry)	0,8	0,40
Gravel (saturated)	1,4	1,80
Asphalt	0,92	0,74–2,88

4.2. Estimation of uncertainty of the laboratory measurement

There always occurs some uncertainty in measurements for many reasons. In this case the main sources for uncertainty were the accuracy of the device, accuracy of PT100 sensors, the sensitivity of the cable, conditions in the laboratory (air conditioning) and human mistake. (Hiltunen, Linko, Hemminki, Hägg, Järvenpää, Saarinen, Simonen & Kärhä 2011).

The accuracy of the DTS device was seen as a key factor for uncertainty in this case. The measurements give two values at the same point in the cable because of the splice in the end of the fiber. Temperature values are given in Table 3 for 10 different points along the multimode cable. For each of these points (D_1, D_2) two corresponding measurements were made (x_1, x_2).

Table 3. Values used in uncertainty calculation.

D_1	x_1	D_2	x_2	x_i	x_i-m_x	$(x_i-m_x)^2$
100	20,37	950	20,38	0,01	-0,53	0,28
140	14,48	910	14,55	0,07	-0,47	0,22
180	18,17	870	16,58	1,59	1,05	1,10
220	20,16	830	20,13	0,03	-0,51	0,26
260	31,05	790	30,63	0,42	-0,12	0,01
300	26,79	750	29,45	2,66	2,12	4,50
340	20,05	710	20,24	0,19	-0,35	0,12
380	20,34	670	20,42	0,08	-0,46	0,21
420	20,14	630	20,32	0,18	-0,36	0,13
460	20,18	590	20,34	0,16	-0,38	0,14
				$\sum(x_i)$=5,39		6,98
		X_i=	$\lvert x_1-x_2 \rvert$	m_x=	0,54	
			Standard	deviation		
			$u_a(xi)$	0,278		**≈0,3**

The standard uncertainty is calculated as a standard deviation of the average temperature differences ($m_{x)}$. To calculate the uncertainty the variance s^2 is needed, which can be counted by Equation 2. Standard deviation is gotten as the square root of variance, Equation 3.

$$s^2(x_i) = \frac{1}{n-1}\sum_{k=1}^{n}\left(x_{i,k} - m(x_i)\right)^2 \quad (2)$$

$$u_{\mathrm{A}}(x_i) = \sqrt{s^2(X_i)} = \sqrt{\frac{s^2(x_i)}{n}} \qquad (3)$$

The standard uncertainty u_A of measurement is ± 0,3 °C. This seems to be quite a good result because the accuracy of ± 0,5 °C was given for the device in the specifications.

Due to the results of estimation of uncertainty it could be decided that in the following inspections of results only one fiber was taken into account and especially measurement points 1, 2 and 3 were noticed.

4.3. Measurements in seabed sediment

In the Suvilahti House Fair area there are two places where the cables were installed at the same time with the heat collection pipes to the sediment in 2008. Temperatures had been measured regularly during the first 14 months but after October 2009 no measurements has been performed (Martinkauppi 2009). Sediment heat is such a new finding that it needs to be researched more precisely and that is the reason to start regular monitoring of sediment heat conditions. This thesis will introduce the first two measurements of this continuous monitoring after three and a half years break.

Sediment heat collection pipes are located in Ketunkatu and in Liito-oravankatu, seen in Figure 13. There is a fan of 14 pipes in Ketunkatu and a fan of 12 pipes in Liito-oravankatu.

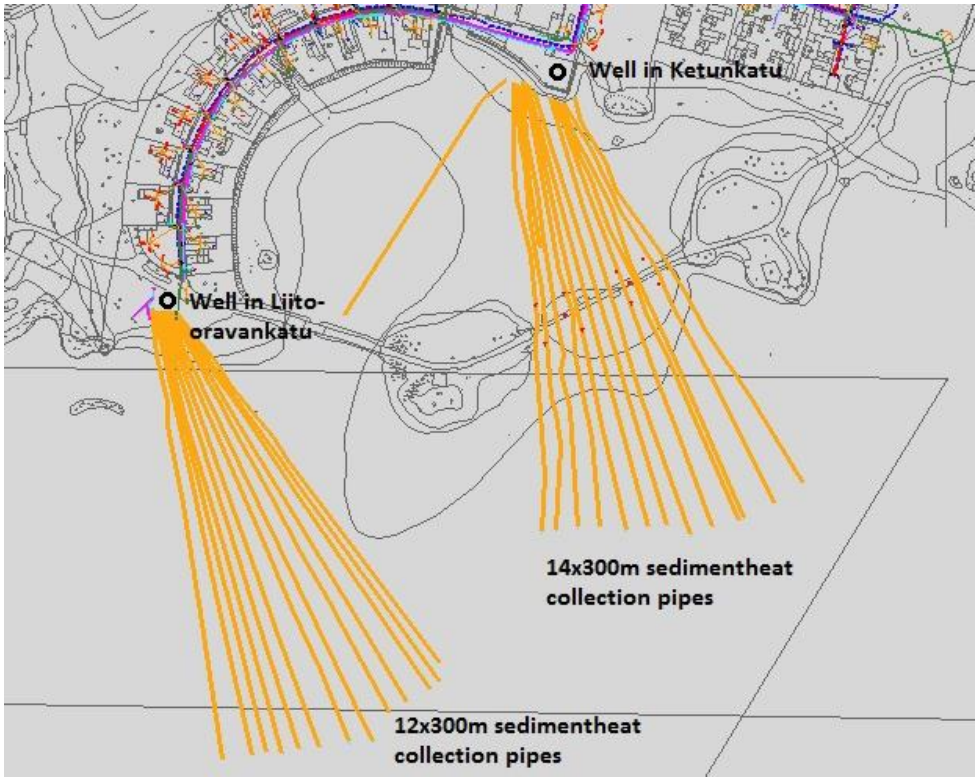

Figure 13. Two sediment energy fields and wells in Suvilahti. (Adapted from Vaasan Vesi 2013).

The heat collection pipes in the Suvilahti seabed sediment are assembled vertically starting from the shore in 0 m and ending to 3–4 meters depth measured from sea level as demonstrated in Figure 14.

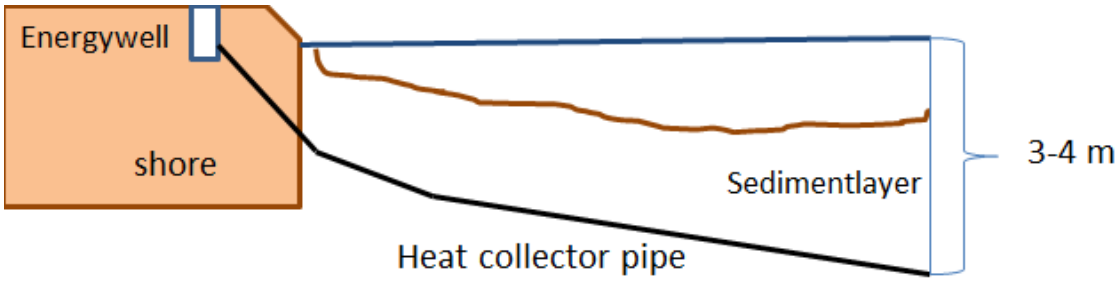

Figure 14. Heat collection pipes are drilled vertically into the sediment layer.

The first measurement took place on the sunny day of March 28th 2013 while the outside temperature was -2 °C. It was still a quite cold time of the year and spring had hardly begun. It was noticed that the well in Liito-oravankatu was full of snow and ice and the measurement could not be implemented on that day. However, the well in Ketunkatu had stayed dry the whole winter and the measurement could be carried out.

The second monitoring measurement was carried out on 30th of April 2013. The outside temperature was +5 °C but the wind was hard and cold. The aim was now to measure both wells, however the well in Liito-oravankatu was still frozen.

The calibration of the measurement was implemented with a calibration box which was filled with a mixture of ice-cubes and water and 142 m of fiber cable (50 µm/125 µm). This cable was also meant to protect the device from dust and dirt in harsh conditions. It can be called a patch cord. The measurement arrangements are shown in Figure 15.

Figure 15. Measurement arrangements made in Ketunkatu on March (left) and April (right), Suvilahti.

In the measurement configuration the spatial resolution was set to 1 m. This measurement was a one-way measurement where the fiber began from the shore and ended in the depth of the sediment. Temperature data was caught from the whole length of the cable.

4.4. Estimation of measurement uncertainty in Suvilahti

In the estimation of uncertainty of the Suvilahti seabed sediment heat measurements there the information about the cable´s location between two projections of heat collector pipe has to be taken into account. In Figure 16 the red arrow points to the location of the cable. The liquid in the heat collector pipe runs in the projections continuously and might have an effect on the temperature monitored from the cable.

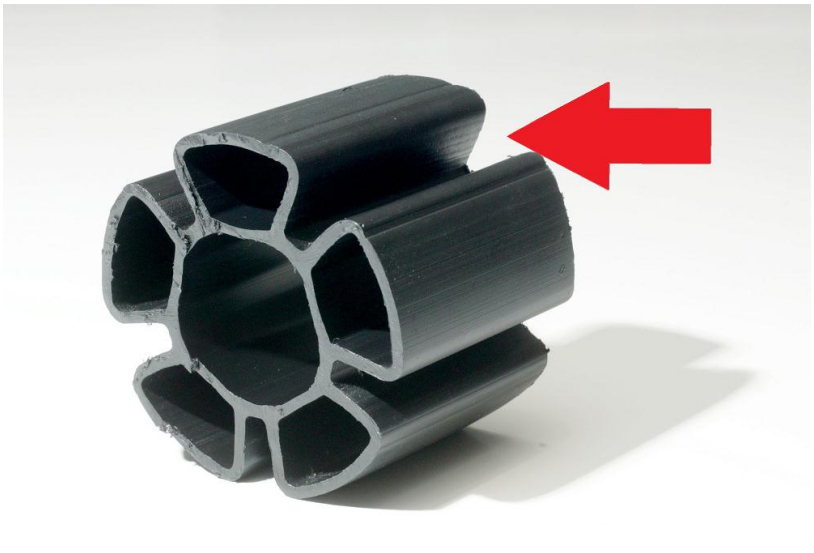

Figure 16. Heat collector pipe with five projections. The red arrow points out the location of the cable. (Adapted from Lieskoski 2013).

On the other hand it is known, according to Martinkauppi 2009, that the excavator has broken the cable at a distance of 37 m measured from the shore and that a section of the cable has been replaced by another cable and it has been spliced together with the original cable at the point of 37 m. The splice can be noticed in the graph, in Figure 17, as a sudden strengthening in signal at the distance of 168 m (arrow 3) which means 168 m-142 m=26m from the shore. This means that the breakage may have been a little bit closer to the shore than reported but in any case there exists a section of replaced cable. Arrow 1 shows the start of the signal from the device. Arrow 2 points out the joint of

patch cord and the fiber in the energy well. The signal is getting stronger after arrow 3 where the fiber has been spliced with another fiber.

Figure 17. Raw data from Ketunkatu on 30.4.2013. Strengthening in signal at 168 m distance in cable (arrow 3). Outside temperature T_{ext2} = 5,12 °C. Temperature in calibration box is T_{ext1} = 0,51 °C.

The loss calculation of signal is shown in Figure 17 also. The loss coefficient is about 1,5 dB/km which is typical value at the wavelength of 975 nm. This wavelength of light is used in Oryx device.

5. RESULTS

The results of the laboratory measurements are presented first. The temperature graphs of the tubs are here presented on an 0,5 °C scale because of the accuracy of the device specified in the specifications. In the end of the chapter the results from the measurements of the real conditions in Suvilahti seabed sediment are shown.

5.1. Measurement point (MP1)/Winter

Measurements in the MP1 tub was started 14.1.2013 at 15:13. Figure 12 shows the temperatures in the tub as a function of distance in the cable a few minutes after the start. The bottom at the height of 115–129 m was filled with warm sand (55 °C, measured just before putting into the tub). Gravel (20 °C) was set next and water (20,3 °C) and ice cubes (0 °C) last. A gradient temperature of about 40 °C was achieved in the tub. Evidently, a connection can be seen between the spatial map of measurement points (Table 1) and the measurement results in the tub (Figure 18). Terms used in the figure texts of the thesis are from now on the following; *t* means time gone after the measurement started, T_{ext1} displays the current room temperature in the laboratory.

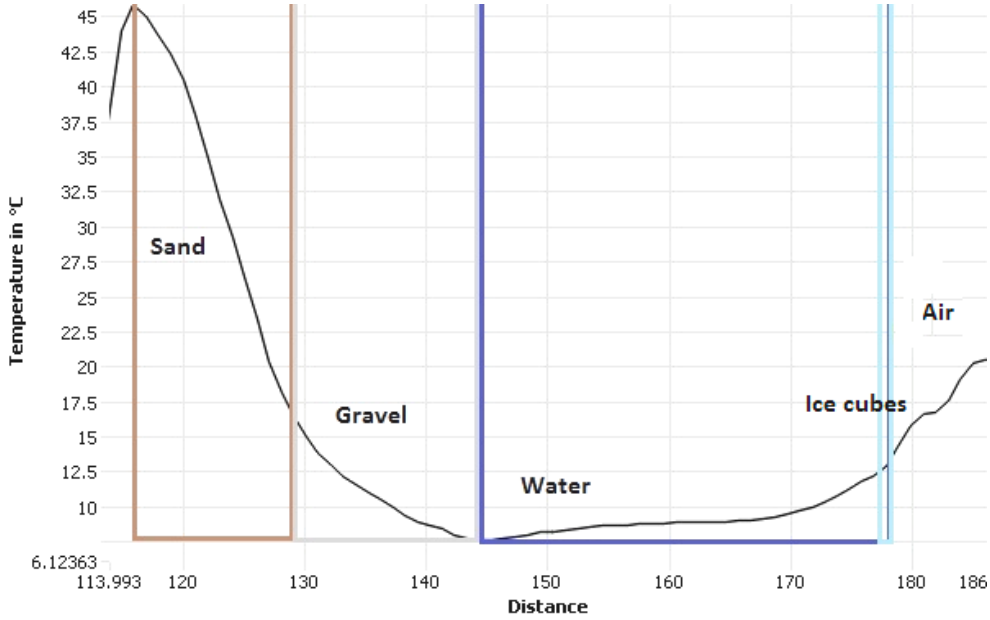

Figure 18. Temperature as a function of distance (m) in the cable in the MP1 tub at the beginning on 14.1.2013 at 15:20. (t=7 min; T_{ext1}=20,51 °C)

After one day of measurements the stabilisation had proceeded quite well which can be noticed in Figure 19. There is an about 5,5 °C difference between the minimum temperature in the tub and the room temperature. The convective heat transfer has occurred naturally, first from the bottom to the top and now from the top to the bottom and it still continues.

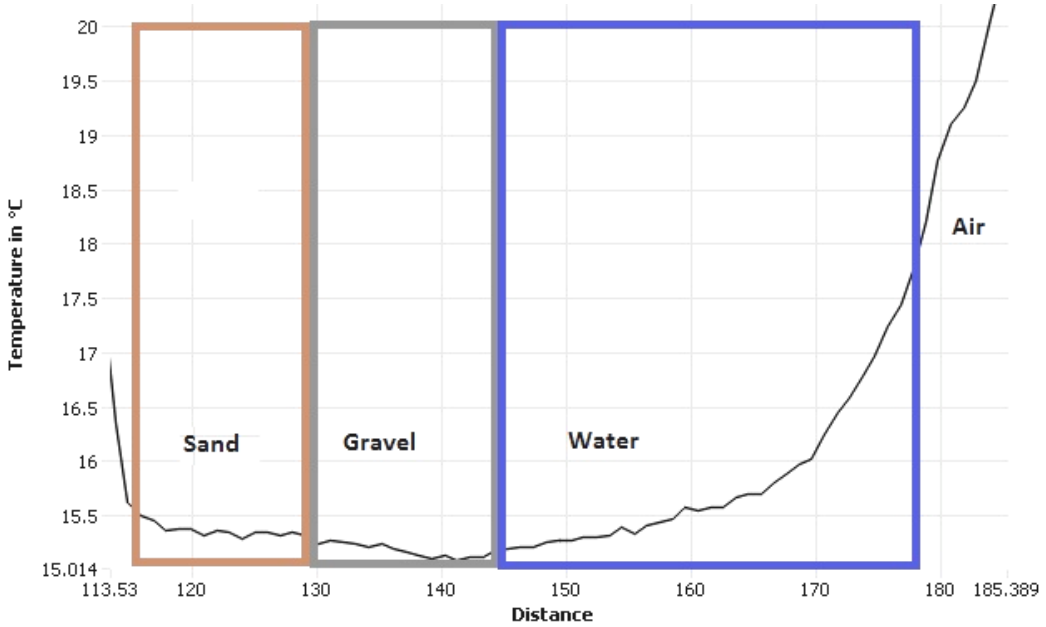

Figure 19. Temperature as a function of distance (m) in the cable after one day stabilisation on 15.1.2013 at 15:20. (t=24 h 7 min; T_{ext1}=20,53 °C)

On the second day after the start there can be acknowledged (Figure 20) that the conditions in the tub are getting warmer and closer to room temperature. Still the difference is approximately 3,5 °C.

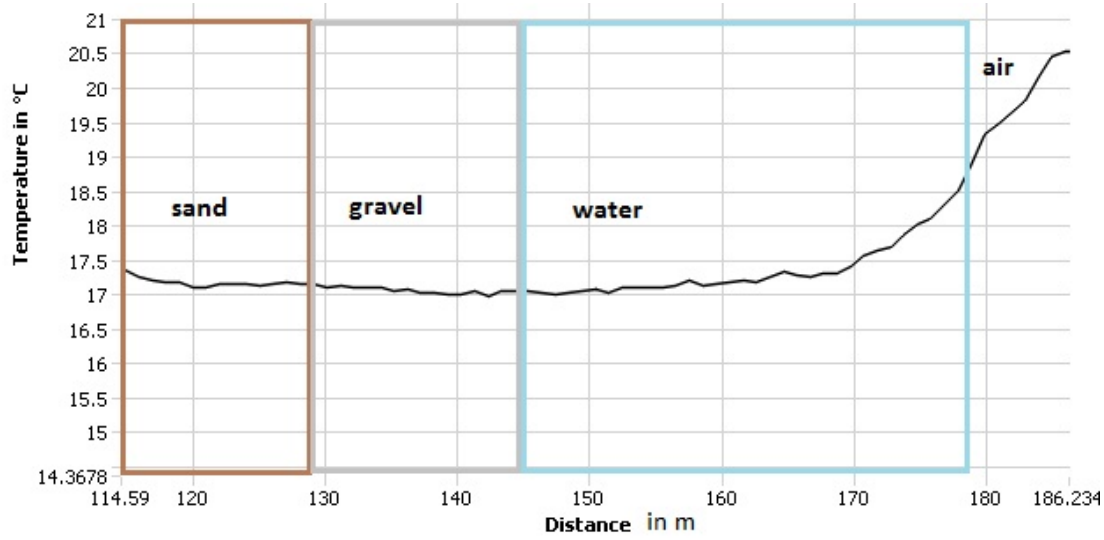

Figure 20. The warming of the tub, temperature as a function of distance (m) on 16.1.2013 at 15:20. (t=48 h 7 min; T_{ext1}=20,56 °C)

After a six days long measurement period there is still an about 1,15 °C difference in temperatures (Figure 21).

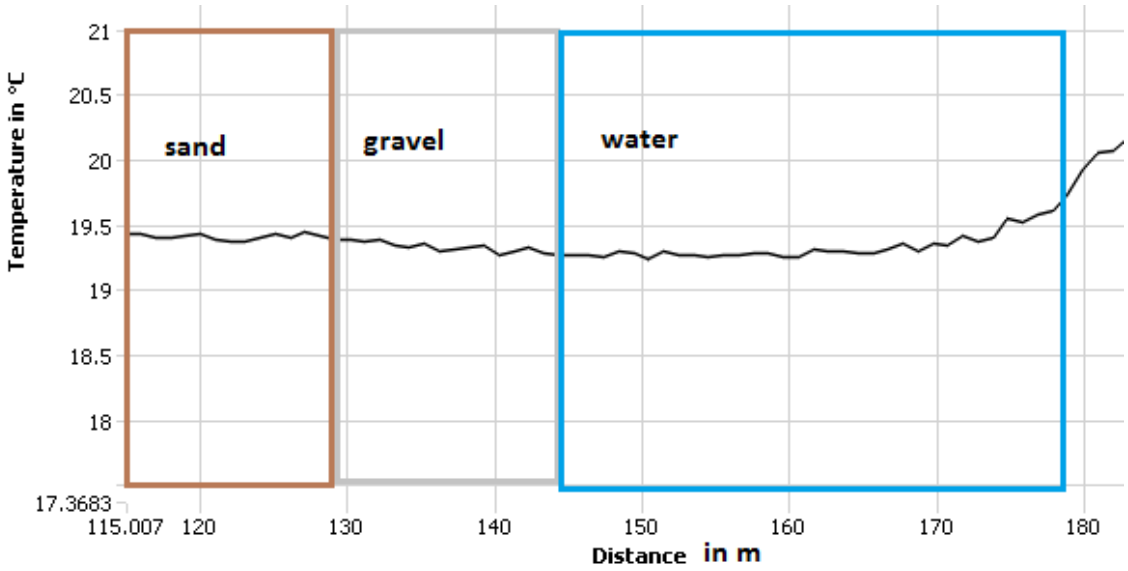

Figure 21. Temperature as a function of distance (m) in the cable on 21.1.2013 at 15:20. (*t*=144 h 7 min; T_{ext1}=20,41 °C)

After 10 days there is still an approximately 1 °C difference between minimum temperature in the tub and the room temperature (Figure 22).

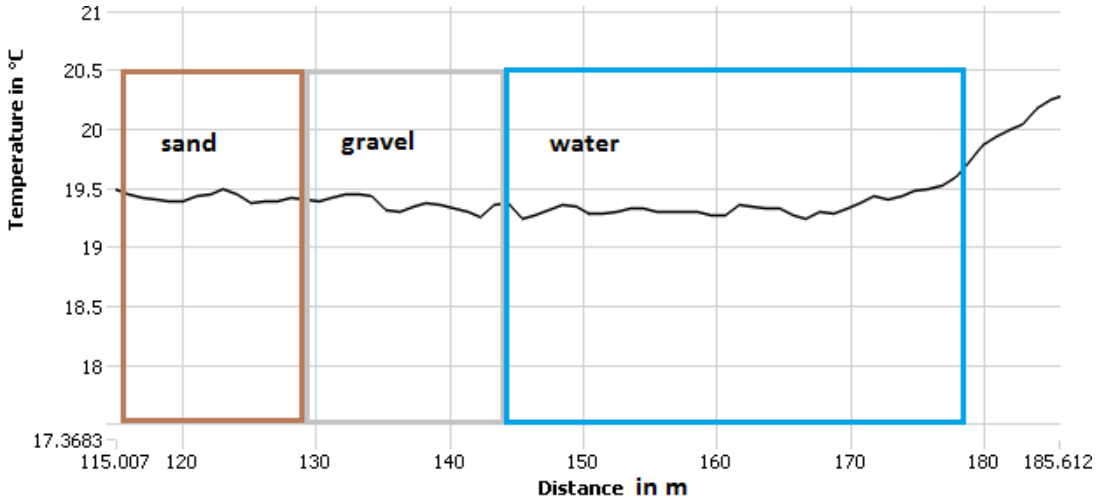

Figure 22. Temperature as a function of distance (m) in the cable on 25.1.2013 at 14:45. (*t*=239 h 32 min; T_{ext1}=20,29 °C)

However, in the evening the temperatures became stabilised (Figure 23). The difference between the temperature in the tub and the temperature in the laboratory is so slight that the measurement could be completed.

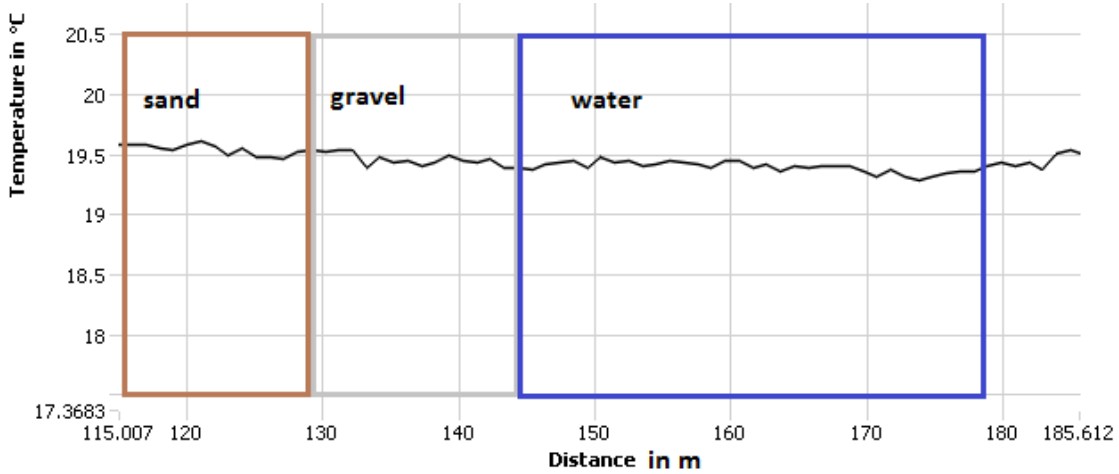

Figure 23. Temperature as a function of distance (m) in the cable on 25.1.2013 at 19:45. (*t*=244 h 32 min; T_{ext1}=19,48 °C)

5.2. Measurement point (MP2)/Summer

The measurement conditions in the MP2 tub was ready on 14.1.2013 at 15:55. Figure 24 shows the temperatures in the tub as a function of distance in the cable five minutes after the start. The bottom was filled with hard ice packs. Next layers consisted of sand and gravel and the tub was filled with warm water (55 °C) to the height of 45 cm from the bottom. There was an about 28,5 °C difference between the maximum temperature in the tub and the room temperature.

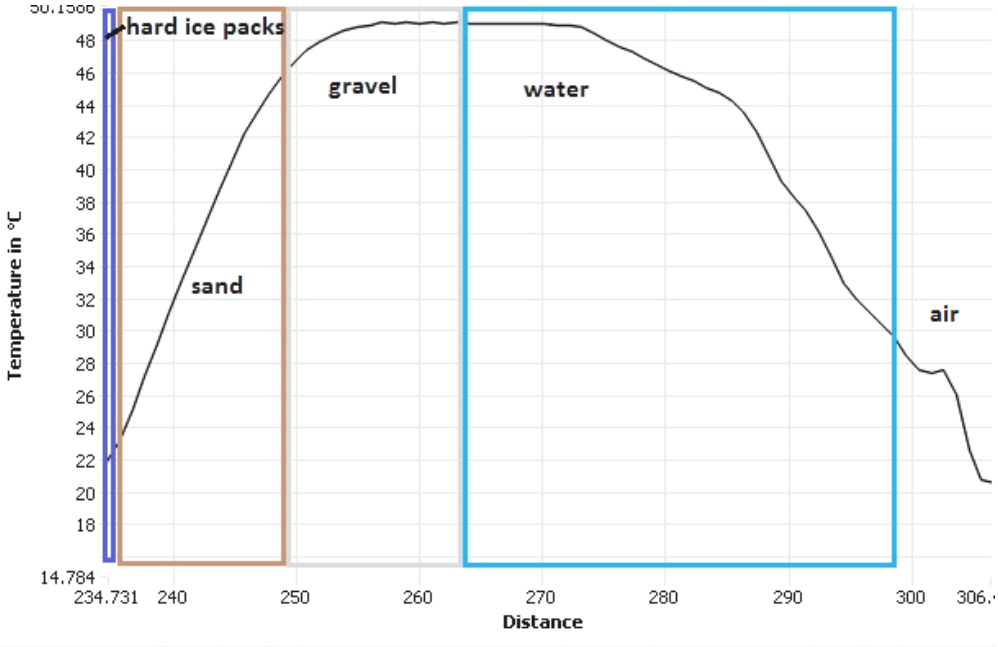

Figure 24. Temperature as a function of distance (m) in the cable in the MP2 tub at the beginning on 14.1.2013 at 16:00. (t=5 min; T_{ext1}=20,52 °C)

After one day of measurements the cooling of the tub has clearly proceeded which can be noticed in Figure 25. The difference is about 7,5 °C.

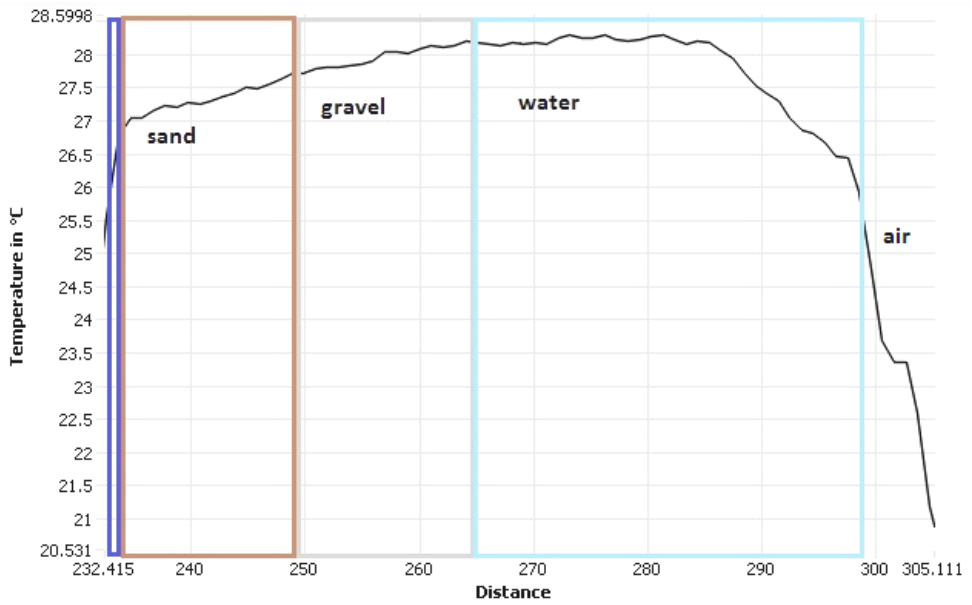

Figure 25. Temperature as a function of distance (m) in the cable on 15.1.2013 at 16:00. (*t*=24 h 5 min; T_{ext1}=20,51 °C)

After 4 days the difference between temperatures in the tub and the room has shrunk to 0,6 °C, see Figure 26 .

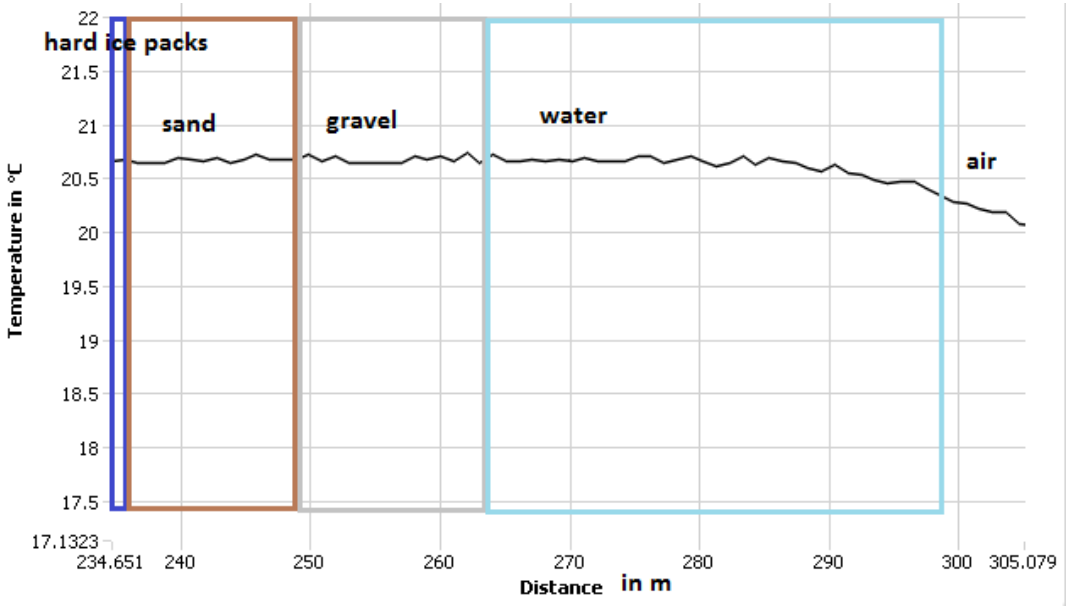

Figure 26. Temperature as a function of distance in the cable on 18.1.2013 at 16:00 (*t*=96 h 5 min; T_{ext1}=20,15 °C)

After six days the conditions are finally stabilized (Figure 27). The difference between the room temperature (19,28 °C) and the average tub temperature (19,70 °C) is so slight that the measurement could be completed.

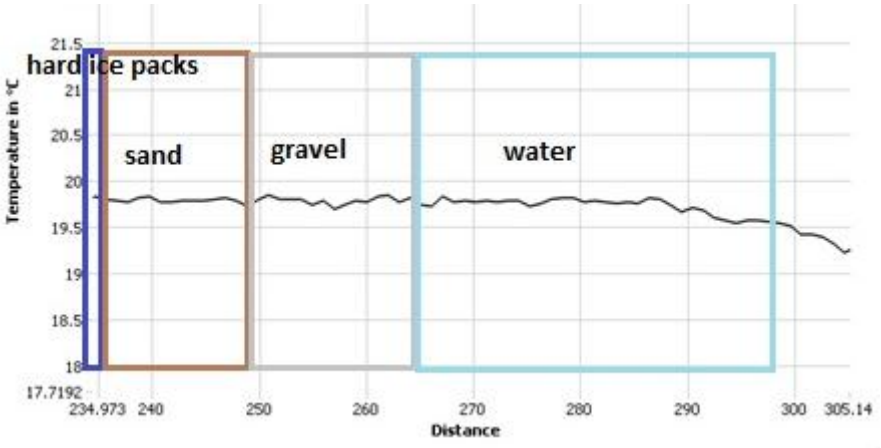

Figure 27. Temperature as a function of distance in the cable on 20.1.2013 at 8:00 (*t*= 136h 5 min; T_{ext1}=19,28 °C)

5.3. Measurement point (MP3)/Dry asphalt

The third measuring tub, MP3, was ready on 15.1.2013 at 8:16. The tub was filled with sand, gravel and asphalt layers. The layers were heated from above by bulb in different periods to simulate the sunlight. MP3 was monitored for a 5 day period, heating the layers during 5–7 hours per day the first 4 days. Figure 28 shows the starting conditions in the tub just a few minutes before the first heating period. The terms used in the figure texts are the following; *t* means time gone after the heating started on that day, T_{ext1} means the room temperature in the laboratory at the moment.

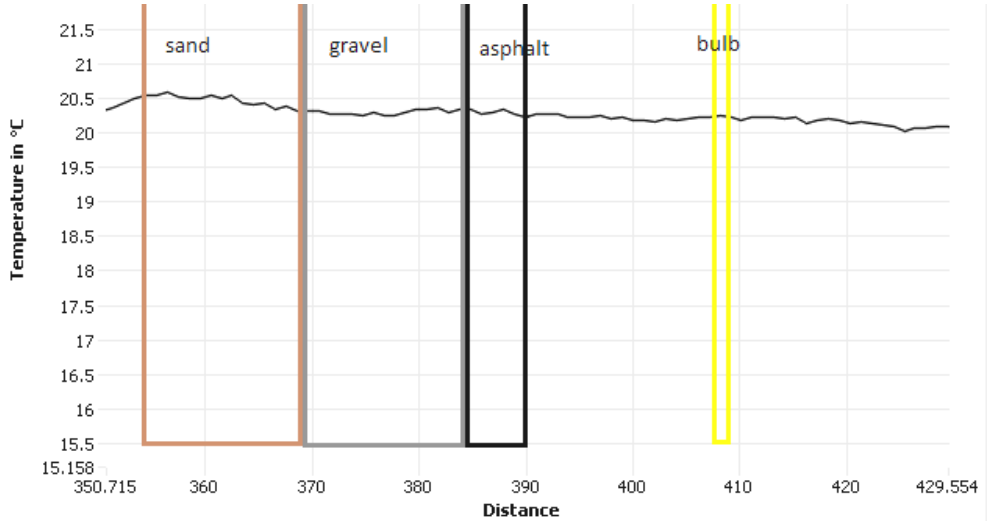

Figure 28. Temperature as a function of distance (m) in the cable in MP3 tub at the beginning on 15.1.2013 at 8:00 (t= 0 min; T_{ext1}=20,06 °C).

On the first day the heating was started at 8:16. In following Figure 29 heating have taken place only for 4 minutes.

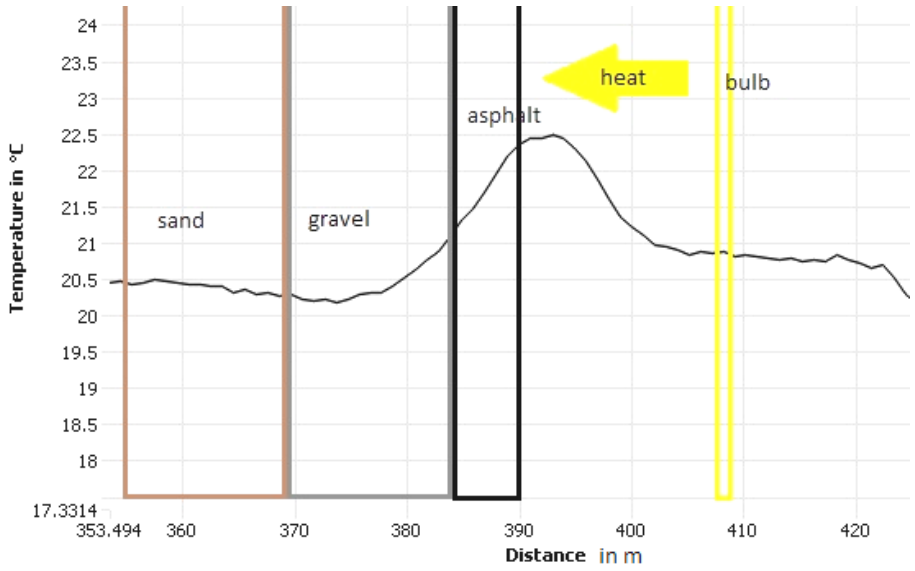

Figure 29. Temperature as a function of distance in the cable in MP3 in the beginning of the heating on 15.1.2013 at 8:20. (t= 4 min; T_{ext1}=20,25 °C)

After approximately 3 hours the heating temperatures have clearly increased as shown in Figure 30.

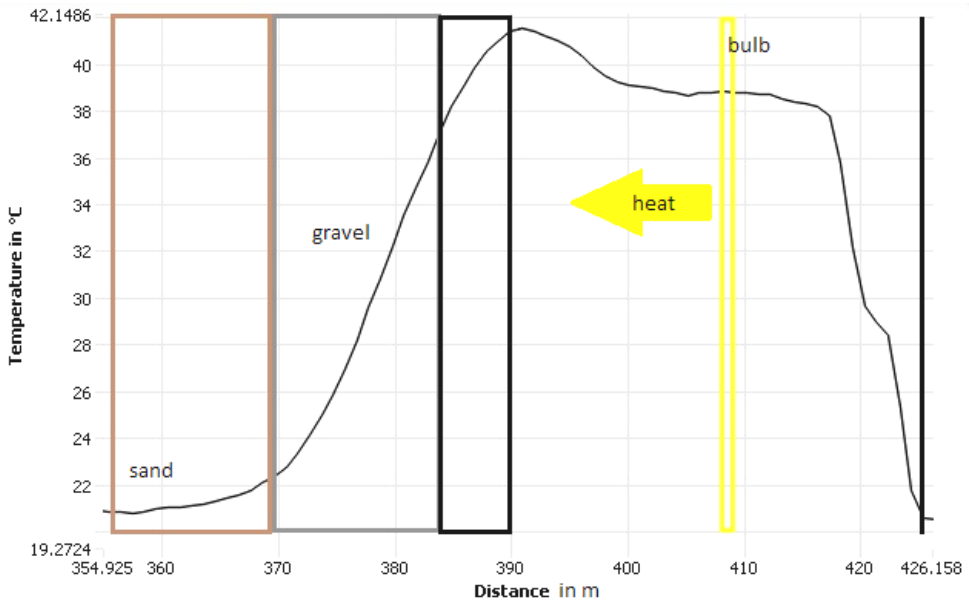

Figure 30. Temperature as a function of distance in the cable in the MP3 tub heating on 15.1.2013 at 11:30. (t=3h 14 min; T_{ext1}=20,53 °C)

The maximum temperatures on the first measurement day of the MP3 tub a few minutes before the end of the heating period are introduced in Figure 31.

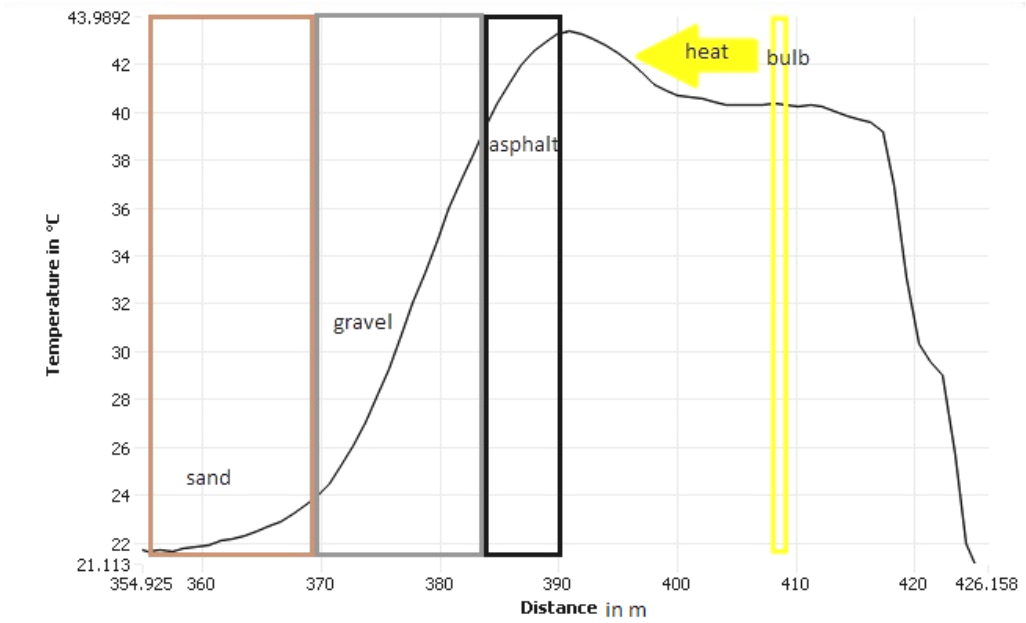

Figure 31. Temperature as a function of distance in the cable in the MP3 tub while heating on 15.1.2013 at 13:20. (*t*=5h 4 min; T_{ext1}=20,57 °C)

Temperatures have fallen to the stage seen in Figure 32 after an 18,5 hours stabilising period.

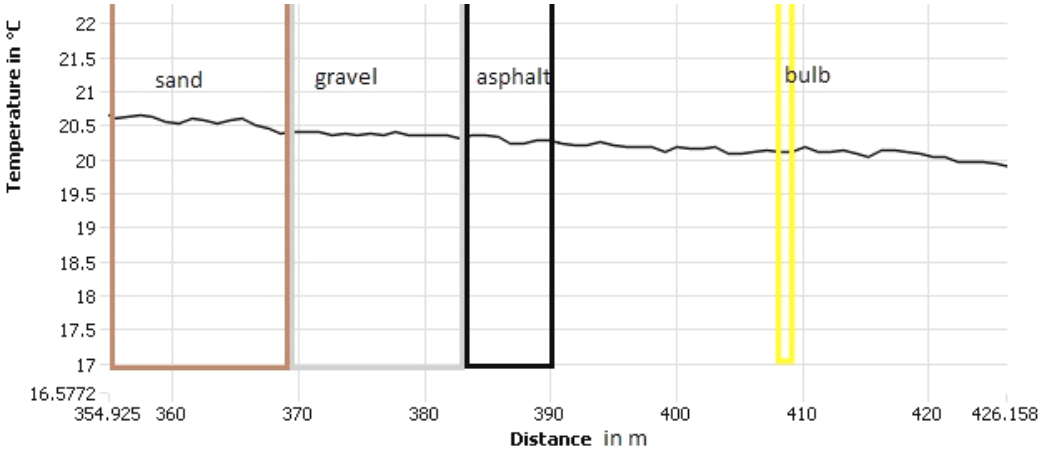

Figure 32. Temperature as a function of distance in the cable in the MP3 tub on 16.1.2013 at 8:00 before the heating period. (T_{ext1}=19,92 °C)

Temperatures after the second day´s heating period are shown in Figure 33.

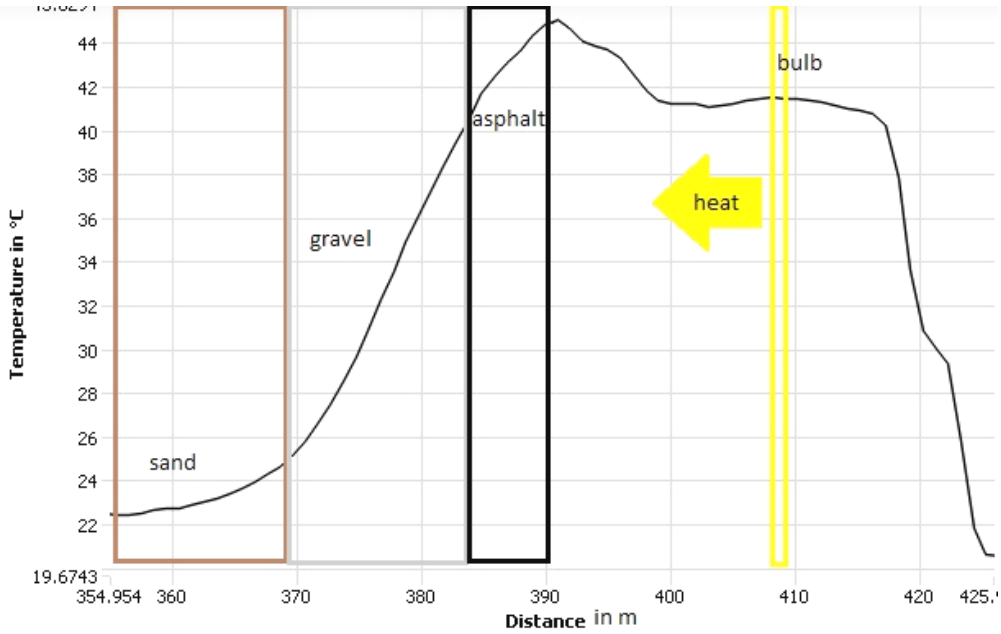

Figure 33. Temperature as a function of distance in cable in MP3 tub on 16.1.2013 at 15:10 after ca. 7 h heating. (T_{ext1}=20,55 °C)

The cooling down of the tub in the evening after the second heating day can be seen in Figure 34.

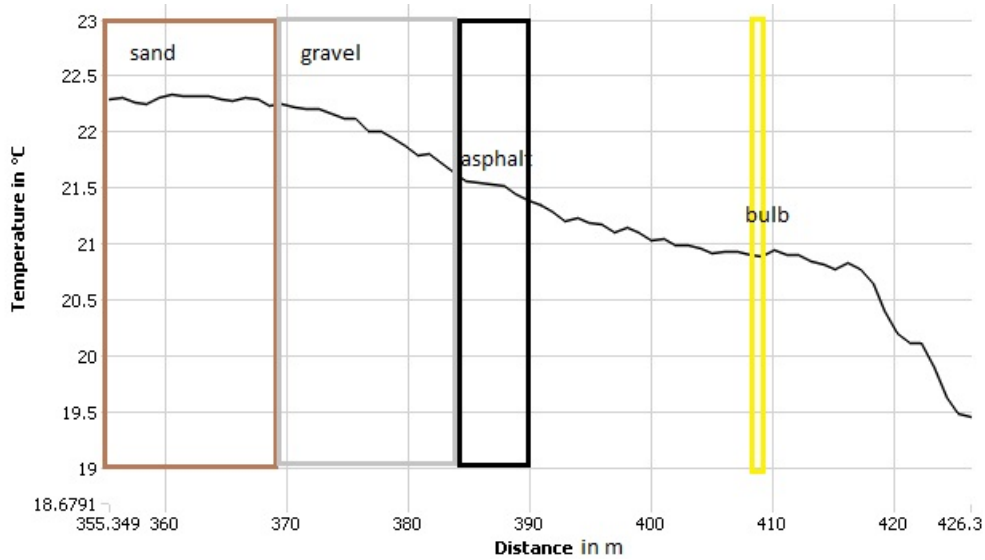

Figure 34. Temperature as a function of distance in the cable in the MP3 tub on 17.1.2013 at 00:00 cooling down. (T ext1=19,63 °C)

In the morning of the third measurement day temperatures were in the stage seen in Figure 35.

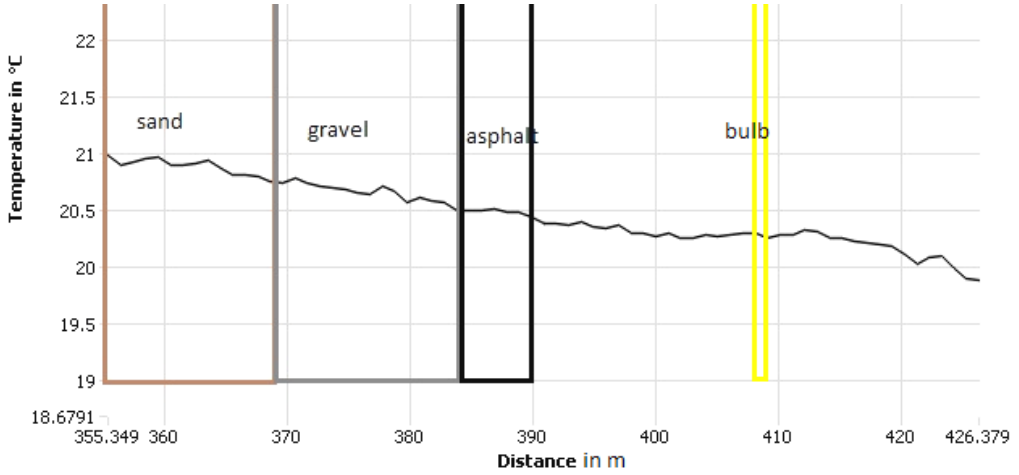

Figure 35. Temperature as a function of distance in the cable in the MP3 tub on 17.1.2013 at 08:00 before heating. (T_{ext1}=20,10 °C)

Temperatures in the end of the third heating period are shown in Figure 36.

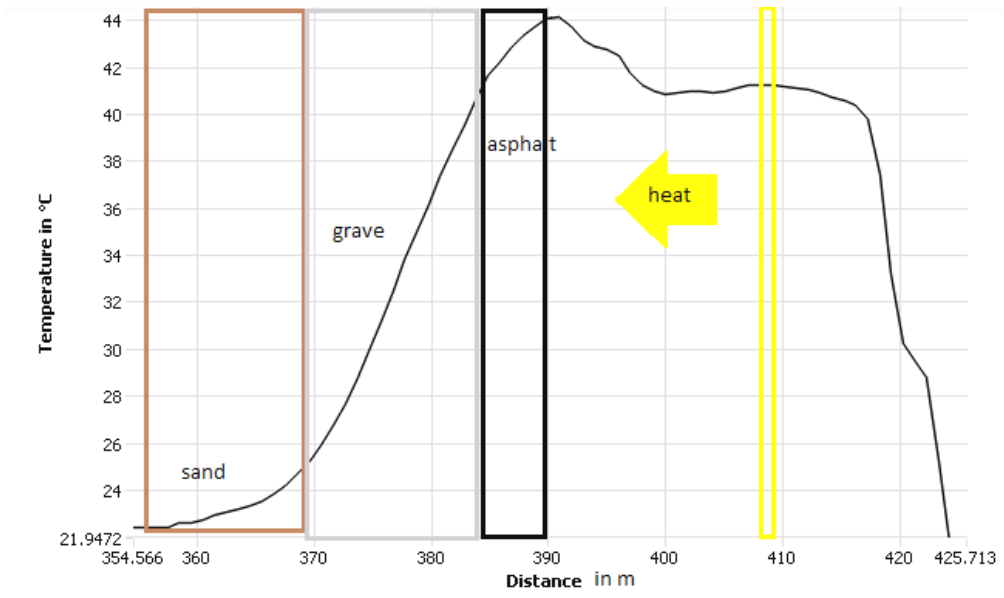

Figure 36. Temperature as a function of distance in the cable in the MP3 tub on 17.1.2013 at 15:30 after 7 h 5 min of heating. (T ext1=20,03 °C)

In Figure 37 the cooling down of materials in the tub can be noticed.

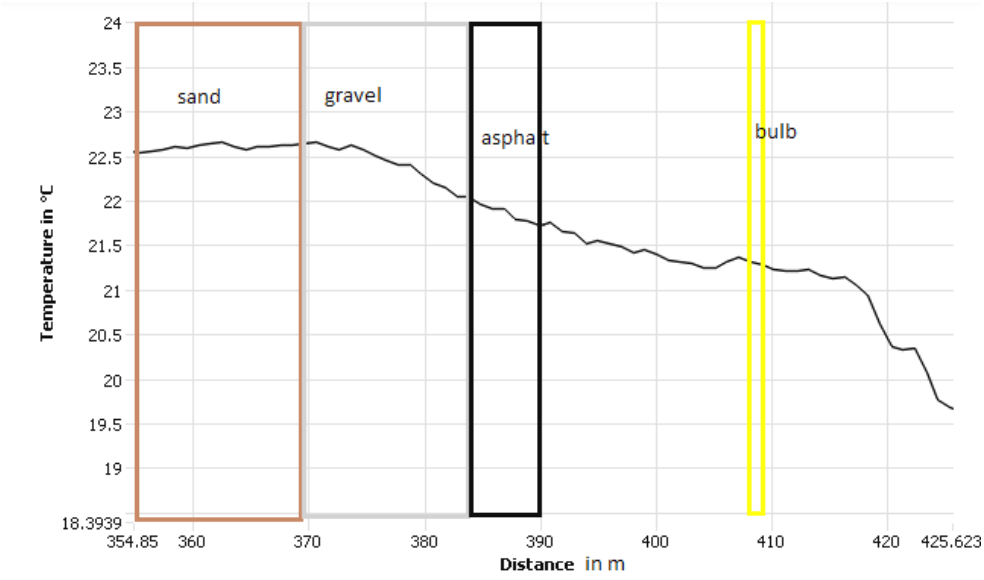

Figure 37. Temperature as a function of distance in the cable in the MP3 tub on 18.1.2013 at 00:00 cooling down. (T ext1=19,76 °C)

The beginning of the fourth and the last heating period took place on 18th of January. In Figure 38 temperatures that are measured a few minutes before switching on the bulb are shown.

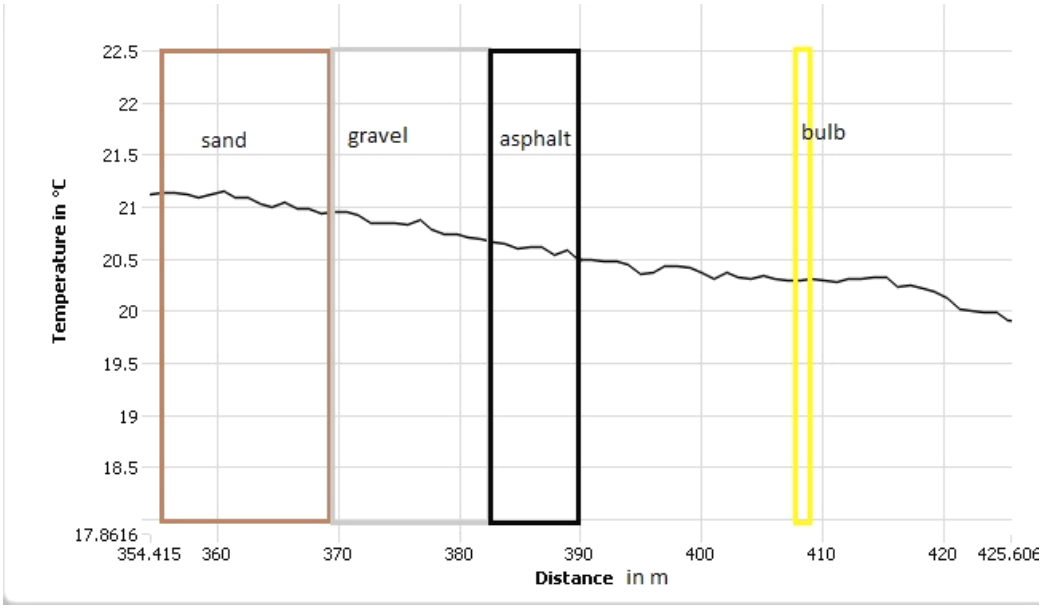

Figure 38. Temperature as a function of distance in the cable in the MP3 tub on 18.1.2013 at 07:40 just before heating. (T ext1=19,89 °C)

In Figure 39 temperatures in the end of the fourth heating period are shown.

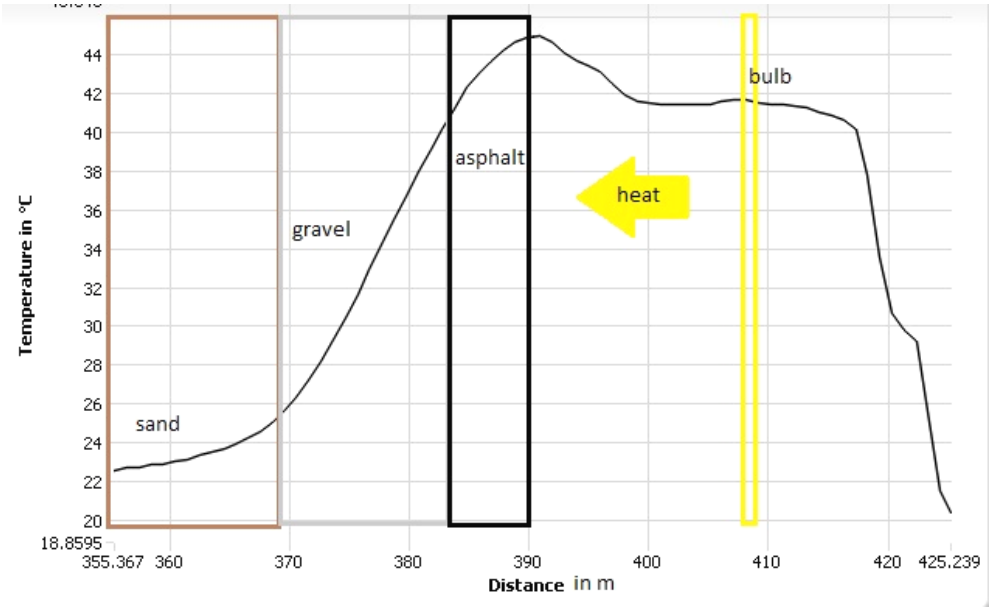

Figure 39. Temperature as a function of distance in the cable in the MP3 tub on 18.1.2013 at 14:50 after 7 h heating. (T ext1=20,02 °C)

At the midnight the cooling down in the tub has proceeded as shown in Figure 40.

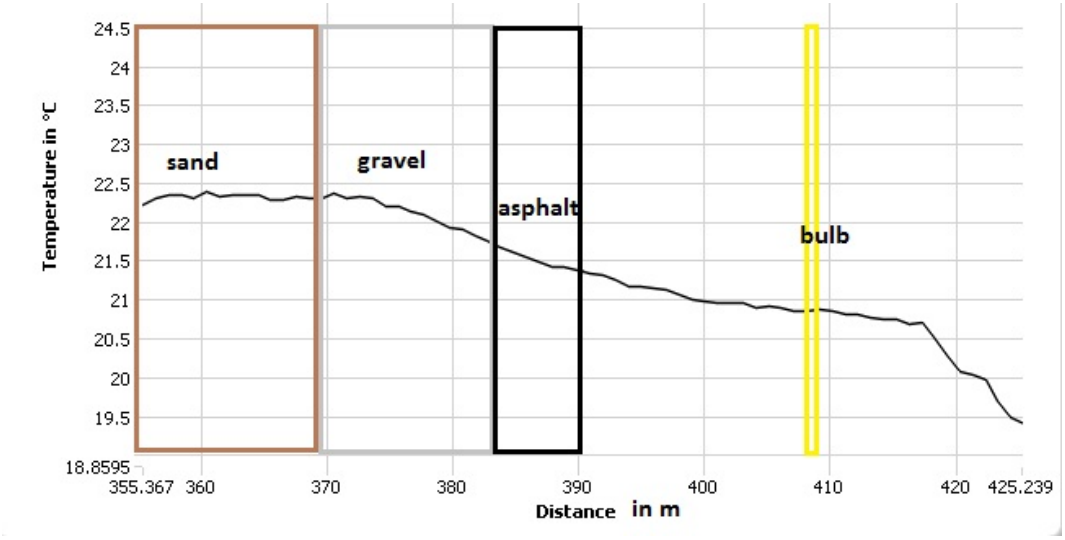

Figure 40. Temperature as a function of distance in the cable in the MP3 tub on 19.1.2013 at 00:00 cooling down. (T ext1=19,45 °C)

In the morning of the next day (19.1.) there still occurs temperature gradient between the tub and the room temperature, Figure 41.

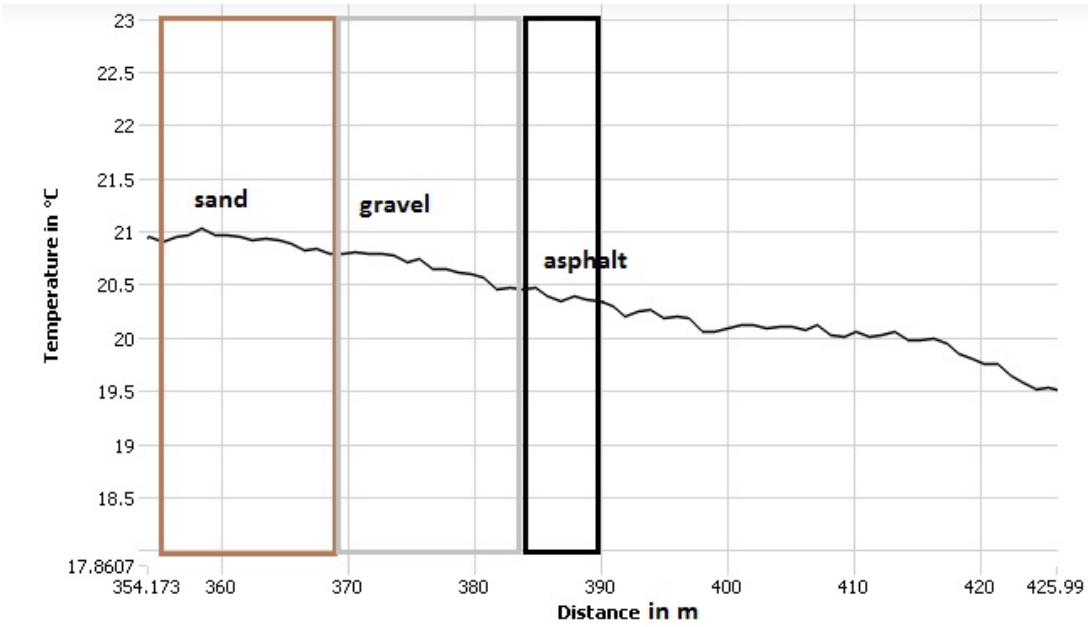

Figure 41. Temperature as a function of distance in the cable in the MP3 tub on 19.1.2013 at 07:00 cooling down. (T ext1=19,48 °C)

A few hours later the temperature in the tub has stabilized seen in Figure 42 close enough the room temperature. The stabilization took 19h 40 min since the last heating period.

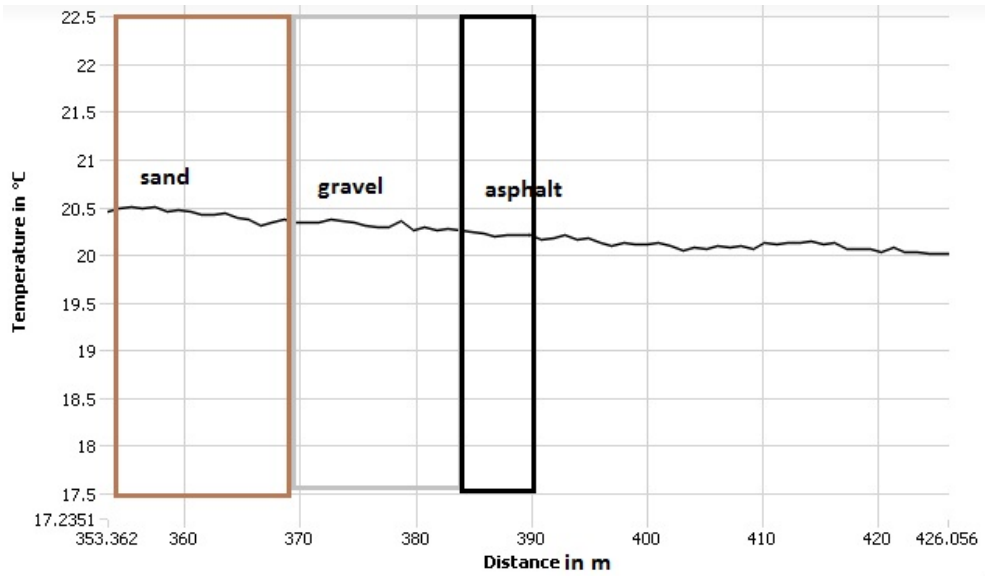

Figure 42. Temperature as a function of distance in the cable in the MP3 tub on 19.1.2013 at 10:30 cooling down. (T ext1=20,03 °C) Variance 0,5. Stabilization has encountered.

5.4. The seabed sediment in Suvilahti

Measurements of the heat in the seabed sediment were implemented on 28th of March and 30th of April 2013. Figure 43 shows the temperatures measured on both days. The starting point on the x-axis is set to the beginning of the fiber in the energy well on the shore.

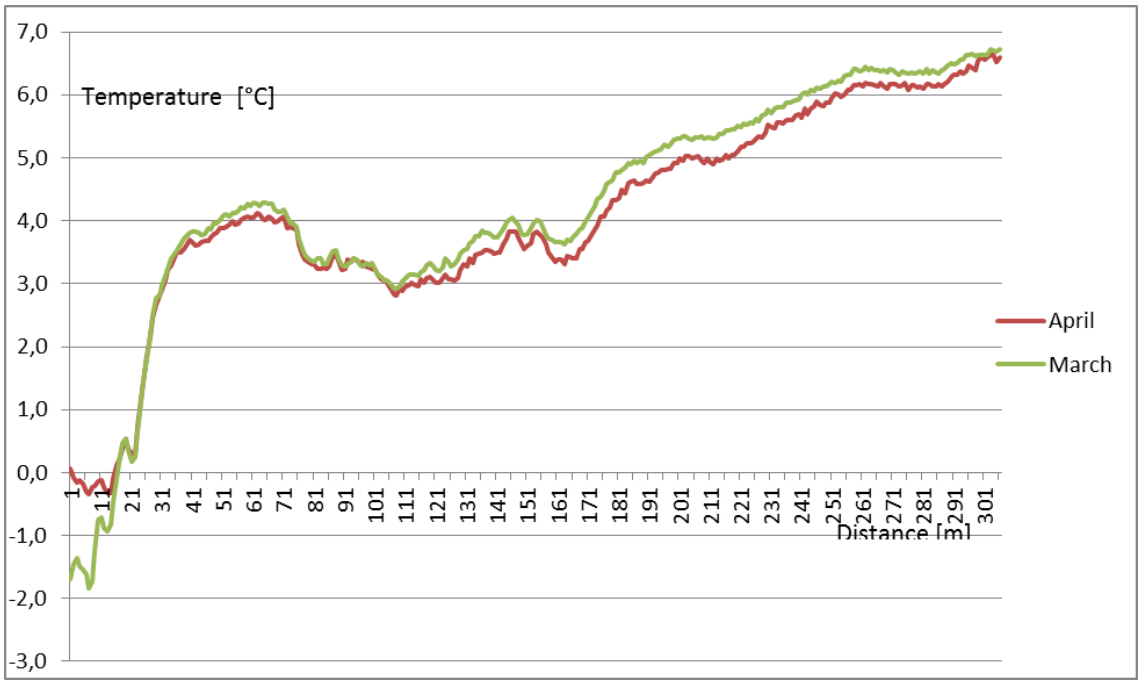

Figure 43. Temperature as a function of distance measured in the seabed sediment of Suvilahti.

In the measurement arrangements the patch cord (0–142 m cable) was used to protect the device from dust and harsh environment. In addition it was set to the calibration box to calibrate the measurement in the seabed sediment. In Figure 44 the temperature in the calibration box (0–142 m) and the temperature in seabed sediment (142–460 m) is viewed for March 28th and April 30th. The calibration box was filled with ice water mixture to reach the stable temperature of 0 °C. As can be seen in Figure 44, this did not succeed perfectly. The PT 100 sensor was used to assure the temperature in the middle

of the calibration box. The sensor measured the temperature of - 0,06 °C in the calibration box in March while the outside temperature was 0,84 °C.

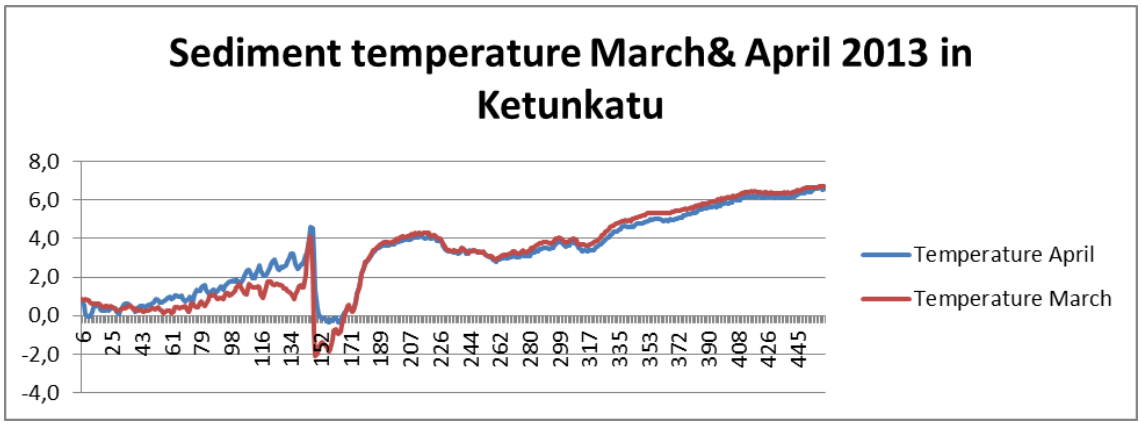

Figure 44. Temperature as a function of distance measured in the seabed sediment of Suvilahti.

6. DISCUSSION

The DTS method is commonly used in the monitoring of bedrock energy wells. In this thesis it was utilized in simulated asphalt conditions and in the seabed sediment. The uncertainty of the laboratory measurements was ± 0,3 °C. It was found quite a good result because the accuracy of ± 0,5 °C was given for the device in the specifications.

In the laboratory measurements the MP1 winter tub stabilized slower than the MP2 summer tub (Figure 45). The temperature in the MP 2 (red line) achieved the room temperature on 20.1.2013 at 8:00, whereas the temperature in the MP1 (blue line) was close to room temperature on 22.1.2013, but reached room temperature first on 25.1.2013.

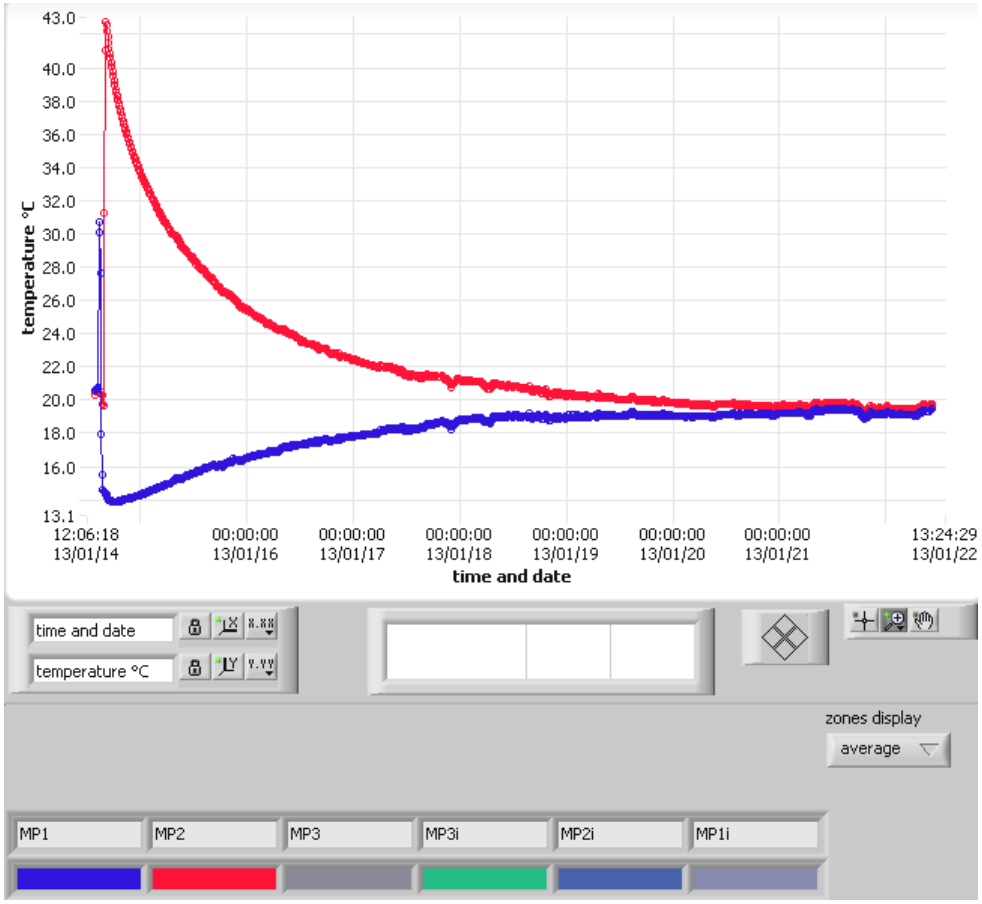

Figure 45. Stabilisation graphs of average temperatures in MP1 (blue line, winter tub) and MP2 (red line, summer tub).

The explanation for this difference in stabilization time is that there in the winter tub there was a gravel layer on the top of warm sand (55 °C) which decelerated the heat convection to the water layer. That happened because the thermal conductivity of gravel (1,80 W/m·K) is lower than sand (2,40 w/m·K), see Table 2. In the summer tub there were no insulating layer preventing the heat convection.

In the MP3 dry asphalt tub measurements it was noticed that asphalt layer binds heat effectively and that heat is conducting to the lower layers, see Figure 46. For example, the temperature in the middle of the sand layer was 20,5 °C at the beginning of the measurements and after four (5-7 h) heating periods the temperature was 23 °C.

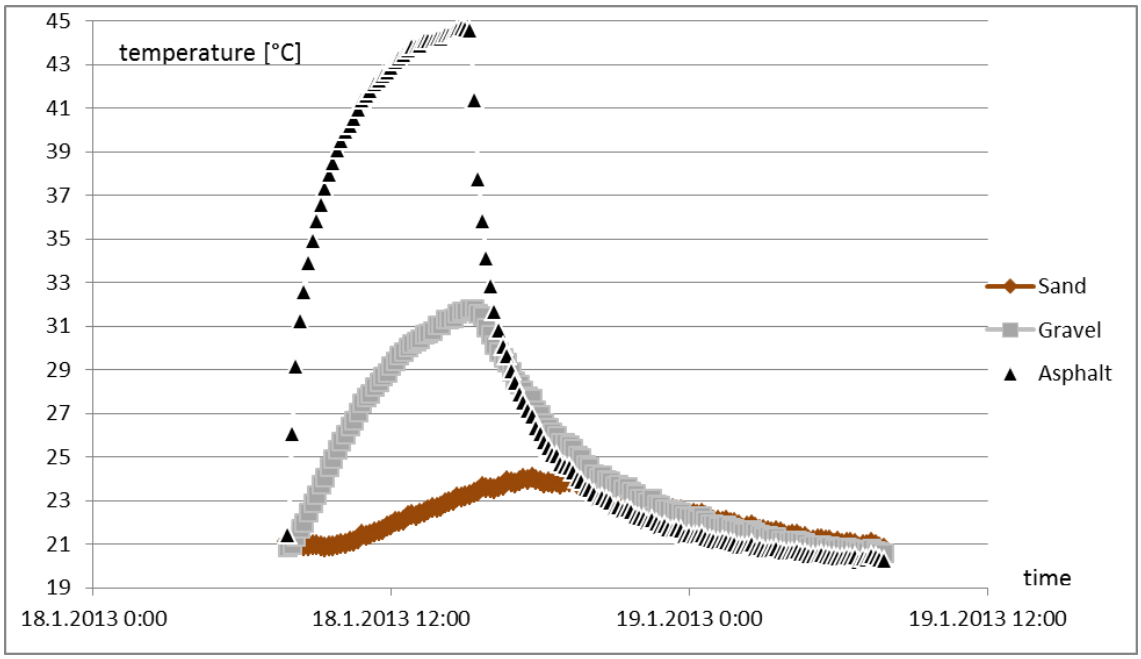

Figure 46. Temperatures in the MP3 dry asphalt tub for one day period.

The experimental set-up in laboratory may have been done more precisely. There could have been more ice in the MP1 Winter tub to more effectively simulate the temperature gradient in winter time. The asphalt pavement should have been done more solid to demonstrate real conditions more precisely. The plastic tub tolerated only the tempera-

ture of 60 °C maximum. In the dry asphalt measurement this has to be taken into account and the heating had to be manually interrupted regularly to control the temperature inside the tub. The use of a thermostat would have been one possibility to control temperature automatically.

The sediment heat graphs, Figure 42, in March and in April are quite similar. The difference is seen only near the shore. Spring has started by the end of April and temperatures have increased a little on the first 15 meters range. In both temperature graphs a drop can be noticed from 4°C to 3°C in 73–178 m distance from the shore. After 178 m the temperature rises little by little to achieve 6,5 °C in the end of the cable at a 300 m distance from the shore.

This kind of shape of curve (Figure 43) can be explained by the exploitation of the sediment energy field. The low-energy network has utilized the energy from the beginning of the heat collector pipes, but in the end of the pipeline there is still available potential. If all houses are getting enough energy, there is a possibility that even a fewer amount of heat collector pipes would have been adequate. According to Aittomäki (2001: 7) Figure 47, this temperature graph can be driven even to 0°C on the whole cable length and still the COP (coefficient of performance) of the heat pumps remains around 3 while the temperature in the liquid of the network is 40 °C. The heat gathering system in the sediment would still serve enough energy for the whole network.

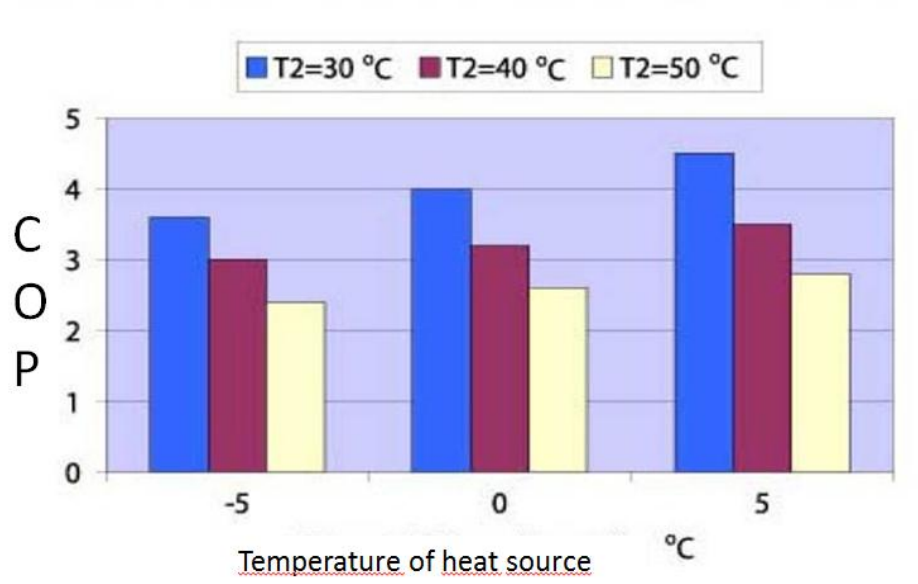

Figure 47. The effect of temperature stages to COP of heat pump. (Adapted from Aittomäki 2001: 7).

The average temperature of the seabed sediment in April is a little bit lower than in March. This result is in accordance with previous measurements made by the Geological Survey of Finland (GTK) in 2008–2009. The Geological Survey of Finland had monitored the sediment heat in Ketunkatu for a 14 months period and the coldest month was April. The shape of the temperature graphs measured by GTK was different than present graphs. That is because of previous measurements represents the beginning of the utilization of the low-energy network. Until the measurements made in this thesis the network has been in use for five years.

In the sediment heat measurements there could have been better calibration arrangements. At least the calibration box should have been insulated better.

7. CONCLUSIONS

The aim of the laboratory measurements was to find out if the device gives accurate temperature data and if the spatial resolution accuracy is reliable. In the laboratory measurements it was clearly noticed that the spatial location of materials was equivalent to the temperatures acquired by the DTS device. The monitoring of simulated winter and summer conditions did manage well. It was possible to execute even several measurements per hour continuously for a one week period and get graphical monitoring data immediately (Figure 45).

The distributed temperature sensing method seems to be an accurate way to monitor temperatures. Ability to monitor even long distance (max 5,3 km in Oryx) is a great benefit of this method. Ranges in geoenergy research are often quite large. The DTS method was found out to be a useful method in asphalt and sediment heat measurements even in the short spatial resolution range.

The DTS method and the results acquired in this thesis will be utilized in further research. The gradients of the temperatures in MP3 dry asphalt tub will be calculated and analyzed carefully. There is a plan to build asphalt measurement arrangements in the parking lot at the University of Vaasa near the Fabriikki building. The DTS method is generally used in the monitoring of energy boreholes but now it will be utilized in the monitoring of temperatures under the asphalt layer in the ground.

8. SUMMARY

The aim of this thesis was to introduce the theory of the distributed temperature sensing (DTS) method, to test it both in the laboratory and in field conditions and to evaluate the results. The asphalt heat measurements were implemented in the laboratory and the sediment heat measurement in the field conditions in Suvilahti, Vaasa.

In the beginning of this thesis the terms geothermal energy, geoenergy, asphalt and sediment heat are introduced. Furthermore the term urban energy is clarified. The laboratory arrangements of the asphalt heat measurement and the arrangements of the sediment heat measurement are introduced and the results are presented. The results are discussed and former results are compared to these new findings.

In the laboratory measurements the MP1 winter tub stabilized slower than the MP2 summer tub. The temperature in the MP 2 achieved the room temperature in six days, whereas the temperature in the MP1 was close to room temperature after eight days, but reached room temperature after 11 measurement days. The MP3 dry asphalt tub was heated to buffer the heat to the asphalt layer and under it.

As a result of this thesis the DTS method is found to be an accurate and modern method which can be utilized in both asphalt and sediment heat measurements. In the Geoenergy project the DTS method is first utilized to monitor temperatures in the seabed sediment and in the soil under the asphalt layer. In the conclusions chapter it is described that the DTS method later shall be used in bedrock energy wells in geoenergy related projects. Regular and continuous monitoring of the temperatures in the seabed sediment was started and documented as a part of this thesis as well.

REFERENCES

Ahvenisto, Ursula, Esa Borén, Sven-Erik Hjelt, Tuija Karjalainen & Jarmo Sirviö (2004). *Geofysiikka. Tunne maapallosi.* (in Finnish) Porvoo: WS Bookwell Oy. 191 p. ISBN 951-0-26113-0.

Aittomäki, Antero (2001). *Lämpöpumppulämmitys.* (in Finnish) Tampere. 22 p.

Allen, Alistair, Dejan, Milenic & Paul Sikora (2003). *Shallow gravel aquifers and the urban ´heat island´ effect: a source of low enthalpy geothermal energy.* Geothermics 32: 569–578.

Aswathanarayana, U., Harikrishnan, T. & K.M. Thayyid Sahini (2010). *Green Energy. Technology, Economics and Policy.* The Netherlands: CRC Press. 341 p. ISBN: 978-0-415-87628-5.

Canbing, Li, Jincheng, Shang & Cao, Yijia (2010). *Discussion on energy-saving taking urban heat island effect into account.* International Conference on Power System Technology POWERCON 2010. IEEE Conference publication p. 1–3.

Chandrasekraham, D. & Jochen Bundschuh (2008). *Low-Enthalpy Geothermal Resources for Power Generation.* United Kingdom: CRC Press. 149 p. ISBN: 978-0-415-40168-5.

Earth Energy Designer EED-program for calculation of boreholes heat exchangers. (2012) Values for soil properties.

Englund Marja, Asko Mitrunen, Pasi Lehtiniemi & Ari Ipatti (2008). *Kuituoptiset anturit siltarakenteiden mittauksissa*. (in Finnish) Report. Fortum Power and Heat Oy. 36 p.

Finnish Meteorological Institute (2010). *Climate Guide.* [Cited 6.11.2012]. Available in World Wide Web: <URL: http://ilmasto-opas.fi/en/>.

Gehlin Signhild E.A. & Bo Nordell (2003). *Determining Undisturbed Ground Temperature for Thermal Response Test.* [Cited 10.5.2013]. Available in World Wide Web: <URL: http://pure.ltu.se/portal/files/1542127/Article.pdf>.

Geoenergia.fi (2010). *Suomalaista maalämpöosaamista.*[Cited 25.8.2012]. Available in World Wide Web: <URL: http://www.geoenergia.fi/ >.

Hiltunen, E., L. Linko, S. Hemminki, M. Hägg, E. Järvenpää, P. Saarinen, S. Simonen & P. Kärhä (2011). *Laadukkaan mittaamisen perusteet.* (in Finnish) Metrologian neuvottelukunta. Espoo. 137 p.

ICAX (2012). *Asphalt Solar Collector*. [Cited 6.8.2012] Available in World Wide Web: <URL: http://www.icax.co.uk/asphalt_solar_collector.html>.

Leppäharju, Nina (2008). *Geophysical and geological factors in the utilization of ground heat*. Master´s Thesis. Faculty of Science. University of Oulu. Oulu.

LIOS Technology (2012). *Distributed Temperature Sensing.* [Cited 8.10.2012]. Available in World Wide Web: <URL: http://www.lios-tech.com/ Menu/ Technology/ Distributed+Temperature+Sensing>.

Lipták, Béla (2009). *Post-Oil Energy Technology. The World`s First Solar – Hydrogen Demonstration Power Plant.* USA: CRC Press. 571 p. ISBN: 978-1-4200-7025-5.

Lowrie, William (2007). *Fundamentals of Geophysics*. 2. Edition. United Kingdom: Cambridge University Press. ISBN-13 978-0-521-85902-8.

Martinkauppi, Ilkka (2010). *Sedimenttilämpömittaukset Pohjanmaalla ja Etelä-Pohjanmaalla.* [Cited 28.11.2012]. Available in World Wide Web: <URL: http://www.geoenergia.fi/pdf/I_Martinkauppi.pdf>.

Martinkauppi, Ilkka (2009). *Vaasan Suvilahden DTS-lämpötilamittaukset.* (in Finnish) Työraportti 18.12.2009. Arkistotunnus Q16.1/2009/76. GTK Länsi-Suomen yksikkö. Kokkola. (not publicly available)

NMC Cellfoam Oy (2013). *Materiaalit.* . [Cited 21.1.2013] Available in World Wide Web: <URL: http://www.cellfoam.fi/nomalen30.html>.

Panula, Erkki-Jussi (2008). *Refla-energiaverkosto tuo merestä lämmön ja viileyden.* (in Finnish) Lähienergiaa. Mateve Oy:n asiakaslehti 1/2008.

Qinwu, Xu & Solaimanian Mansour (2010). *Modeling temperature distribution and thermal property of asphalt concrete for laboratory testing applications.* Construction and Building Materials 24: 487–497.

Quimby, Richard S. (2006). *Photonics and Lasers. An Introduction.* USA: Wiley Interscience. 519 p. ISBN-13 987-0-417-71974-8.

Rosén Bengt, Anna Gabrielsson, Jan Fallsvik, Göran Hellström & Gunnel Nilsson (2001). *System för värme och kyla ur mark–En nulägesbeskrivning*. (in Swedish) Staten geotekniska institut (SIG). Varia 511. Sweden: Linköping. 236 p.

Santamouris, M. (2003). *Solar thermal technologies for buildings–the state of the art.* United Kingdom: Cromwell Press. ISBN-1-902916-47-6.

Sayde, Chadi, Christopher Gregory, Maria Gil-Rodriquez, Nick Tufillaro, Scott Tyler, Nick van de Giesen, Marshall English, Richard Cuenca & John S. Selker (2010). *Feasibility of soil moisture monitoring with heated fiber optics*. Water Resources Research 46: 1-8.

Sensornet (2007). *Oryx DTS User Manual v4*. United Kingdom. 101 p.

Smolen James J. & Alex van der Spek (2003). *Distributed Temperature Sensing. A DTS Primer for Oil & Gas Production.* Shell EP2003-7100 May 2003. Craphics Team P03885. 76 p.

Ukil Abhisek, Hubert Braendle & Peter Krippner (2012). *Distributed Temperature Sensing: Review of Technology and Applications.* IEEE Sensors Journal 12: 5, 885–892.

Valpola, Samu (2006). *Sedimentin lämpötilamittaukset Vaasan Suvilahden edustalla.* (in Finnish) Arkistoraportti P31.4.053. GTK Länsi-Suomen yksikkö.

Valtanen, Esko (2007). *Matematiikan ja fysiikan käsikirja.* (in Finnish) 2.painos. Jyväskylä: Genesis-Kirjat Oy. 381 p. ISBN: 978-952-9867-28-8.

APPENDICES

APPENDIX 1. Sediment heat temperature graph including the patch cord

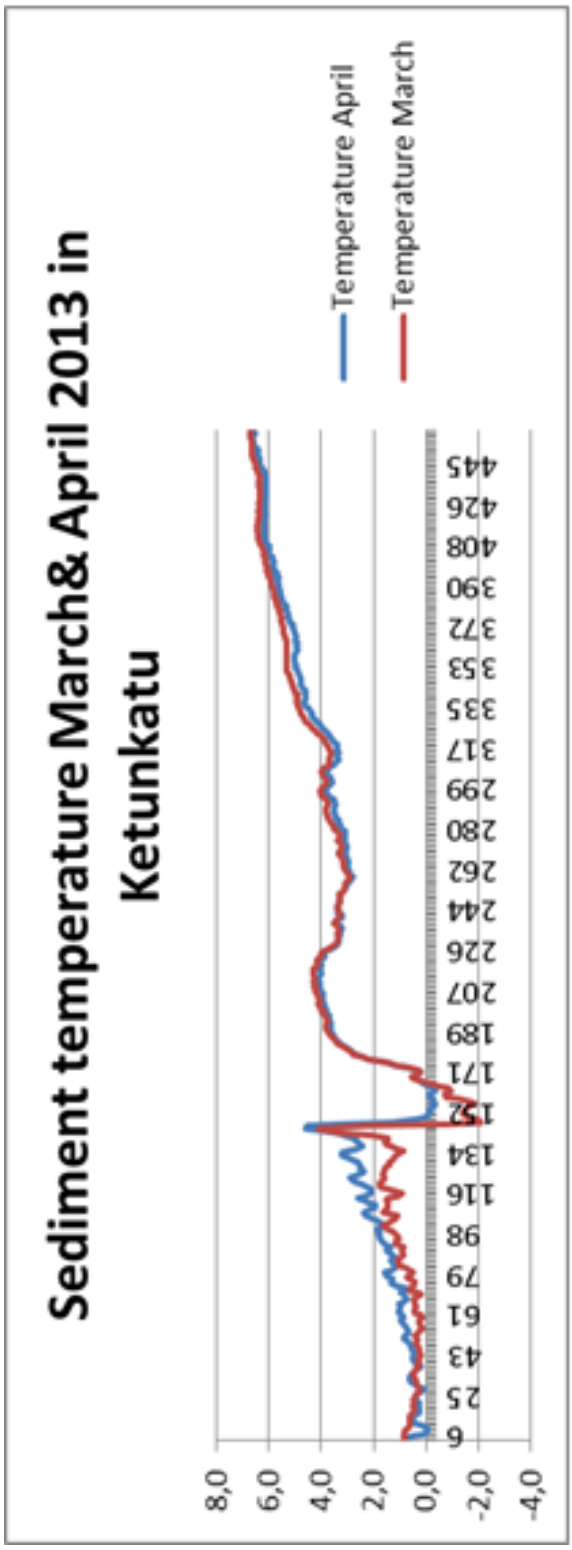

APPENDIX 2. Sediment heat temperature graph starting from the shore